JOURNAL OF FOREST SCIENCE, *48*, 2002 (2): 49–69

The elasto-mechanical behaviour of Douglas fir, its sensitivity to tree-specific properties, wind and snow loads, and implications for stability – a simulation study

D. GAFFREY[1], O. KNIEMEYER[2]

[1]*University of Göttingen, Faculty of Forest Sciences and Forest Ecology, Institute of Forest Biometry and Informatics, Göttingen, Germany*
[2]*University of Göttingen, Faculty of Physics, Institute of Theoretical Physics, Göttingen, Germany*

ABSTRACT: A full 3-D model was developed to simulate the elasto-mechanical behaviour of trees subjected to wind and gravitational forces with the aim of estimating the stress and strain distribution at the surface of the stem. The model was adapted to geometry and material properties of a 64-year old Douglas fir tree. The results are comparable, on the whole, with those of a finite element model of this tree. Original stem and crown data, as well as the applied forces, were modified manifold in order to study their importance on the change in fibre stress and thus, on the safety reserve against stem breakage.

Keywords: Douglas fir; elasto-mechanical model; stress; strain; safety reserve; stem breakage

The stability of single trees and of entire forest stands against wind-induced damage, such as stem breakage and uprooting, has been an intensely studied subject for many years (e. g., BARGMANN 1904). Recent storm disasters gave rise to an integrated, international expert exchange (conference on wind and wind-related damage to trees in Edinburgh, 1993: COUTTS, GRACE 1995; conference on wind and other abiotic risks to forests in Joensuu, 1998: PELTOLA 2000). One outcome is a stand risk simulator, freely accessible on the Internet [*] ("STORMS project demonstrator": MILLER et al. 2000). Uniting different models that account for the relations between wind forces and the mechanical reactions of trees (ForestGALES: QUINE 1998; GARDINER, QUINE 2000); HWIND: PELTOLA et al. 1999; TALKKARI et al. 2000; and models of VALINGER and FRIDMAN (1997; FRIDMAN, VALINGER 1998), the risk either of breakage or turn-over can be estimated in dependence on site-, stand- and tree-related characteristics, which will allow deriving damage preventive decisions.

Apart from economically based management interests in the mechanical failure of trees, mechanical aspects are also of fundamental biological concern, especially the physical properties of the stem which highly contribute to the ability of a tree to come out on top against its competitors (MOSBRUGGER 1990; NIKLAS 1992). Further, plants can change their mechanical properties in the course of their ontogenetic development in order to cope best with the particular prevailing living conditions (SPECK 1994; SPECK et al. 1996; STERCK, BONGERS 1998). Aspects of mechanical stability and approaches to quantify and evaluate the safety of trees have been widely discussed (MCMAHON, KRONAUER 1976; KING, LOUCKS 1978; KING 1986; MATTHECK 1991; NIKLAS 1994; NIKLAS, SPATZ 1999), and hypotheses of adaptive growth and of stress and strain constancy of a stem bent by wind forces were set up (METZGER 1893; TIRÉN 1928; YLINEN 1952; WILSON, ARCHER 1979; MATTHECK 1990).

Basically, responses to questions on this subject are to be obtained by experimental work, e. g., by simultaneously measuring wind speed and fibre strain at the surface of the bent stem (BLACKBURN 1997; BLACKBURN, GARDINER 1997) or by destructively sampling the tree (NIKLAS, SPATZ 2000). As such work is by nature very laborious and often tedious, in this context, a versatile tool is desirable for detailed modelling of the architecture and the mechanical properties of a tree, and to simulate its elasto-mechanical reactions caused by defined wind and gravitational forces. By modifying tree-related parameters or

[*]http://bamboo.mluri.sari.ac.uk/storms

acting forces, an exhaustive study of the sensitivity on the observed effects, firstly, the experienced stresses and strains, can be performed.

As existing models usually show deficiencies in representing naturally built trees and realistic acting loads, a basic demand is to take into account the inhomogeneous distribution of the wood density and of the Young's modulus within the stem, as well as a crown spatially resolved into (first-order) branches (FOURCAUD, LAC 1996) and wind forces distributed according to the crown sail area (SPATZ, BRÜCHERT 2000; NIKLAS, SPATZ 2000). Additionally, the form of the stem cross section should enter the model, as the contribution of the form of the stem to its flexural stiffness is of great importance (SPECK et al. 1990; NIKLAS 1992).

In compliance with these demands, in a first approach, the finite element method (FEM) was applied to model a 64-year old Douglas fir tree including the acting forces (GAFFREY et al. 2001). As this model type turned out to be unhandy to variously realise changes of input parameters for sensitivity studies and because of some model-inherent weaknesses, another differential equation approach was chosen, in which the object is "holistically" defined (SLOBODA, GAFFREY 1999; GAFFREY 2000), contrary to the finite elementary formulation.

First, this paper introduces the underlying theory of elasto-mechanics especially adapted for a stem considered to be a compound material with spatially inhomogeneous material properties and with an irregular cross-section form, and gives the mathematical formulation of the differential equation problem and its solution. Secondly, as strain measurements during bending of the tree were not performed and thus, data for verifying the simulation results do not exist, it is tested – to exclude significant model bugs – whether the prognostications of the finite element model (FE model) coincide with those of the holistic model (which was named TREEFLEX). Third, referring to the results based on the original tree data and on a certain assumed wind profile, TREEFLEX was applied to estimate and evaluate the effects on stress change by varying crown structure, stem form and stem material characteristics, wind profiles, and by additional loads.

MATERIAL AND METHODS

A 64-year old Douglas fir tree, 29.55 m in height and with a dbh of 34.2 cm (without bark), coming from a pure stand located at Esbeek in the southern Netherlands, was destructively sampled in order to measure and estimate respectively, the masses of stem, branches and needles, the crown structure and sailing areas, the inner stem geometry and the spatial distribution of wood density and Young's modulus within the stem. (Further four neighbouring trees were examined, but as data are not presented here, for details see SLOBODA and GAFFREY [1999; GAFFREY, SLOBODA 2001].) In order to calculate wind forces, a typical storm condition was defined and a certain theoretical static wind profile assumed. The tree and load model which is based on these very data serves as a reference when modifications of either tree-specific or wind-related parameters are made. (Some data and illustrative demonstrations have been published on the Internet,** which will be indicated in the following.)

STEM GEOMETRY AND WOOD PROPERTIES

A stem analysis was performed by exactly digitising each year ring of 28 disks, the first one taken at a height of 0.4 m and the last at 27.0 m. In the model, 36 co-ordinates per ring, equidistantly spread, were used (data on the Internet). The total volume, excluding bark, was about 1.16 m^3.

Concerning the wood properties, it has to be stated that only the bulk density of oven-dry disks was actually measured. Thus, the estimated dry mass of the total stem was 639 kg and about 920 kg for fresh mass. As Douglas fir shows a typical, species-specific pattern of altering its wood density from ring to ring, starting with high values near the pith, a minimum at about the tenth year ring and an increase towards the peripheral rings, a corresponding density function was assumed to be valid for this tree, too, and was fitted for each stem disk (GAFFREY et al. 1999).

$$\rho_8(k,\Delta\rho_i) = \frac{-6.33}{(k-10)^2+69.86} + 0.6 + \Delta\rho_i \quad (g/cm^3) \qquad (1)$$

It is $\rho_8(k,\Delta\rho_i)$ the wood density, at a moisture content of 8%, depending on the cambial age k, which is given by the ring number with the count beginning at the pith, and a shift term $\Delta\rho_i$ that accounts for the difference between disk-specific density and mean density. Regarding a specific year ring, the wood density between two neighbouring stem disks was assumed to be constant. The density of the year ring in this section was calculated by averaging the ring-related densities of both disks, weighted by the cross-sectional areas of the rings. The density of fresh, green wood was estimated by assuming the moisture content of the heartwood and sapwood, adopting mean literature values, to be 30% and 120%, respectively, and to take account of the swelling. Due to modelling constraints, instead of the real sapwood area, for all stem disks, the outer ten year rings were considered as the water-conducting rings.

Derived from the wood density was the modulus of elasticity (MOE) E^* by applying published regression functions (PALKA 1973), in modification (GAFFREY et al. 1999).

$$E = E^*(\rho_{u\cdot}/\rho^*_{u\cdot})\cdot[1 + a\cdot\Delta u],\ \Delta u = \min[(u-u^*), u_{max}] \qquad (2)$$

E^* is the MOE at a reference density $\rho^*_{u\cdot}$ with moisture content u^*, a is –0.01 (PALKA 1973) and u_{max} = 24% is the estimated limit moisture content, above which the mechanical properties of Douglas fir wood are no longer affected.

**http://www.uni.gaffrey.de (see page "Demos/Downloads")

Taken from literature (KOLLMANN 1951), for this Douglas fir tree, the MOE was assumed to be 11.5 GPa at a bulk density of 0.5 g/cm^3 and at a moisture content of 12%. Corrections for the moisture content of green wood were made.

Thus, due to the chosen model, the three-dimensional variation of the MOE follows that of the wood density. But it must be stated that this relation, though valid for Douglas fir in general, probably does not match the characteristics of this individual tree (NIKLAS 1997).

The finite element model of the stem (GAFFREY et al. 2001), too, is based on the data and assumptions described above, but some differences in geometry and wood properties must be outlined: each year ring is defined by only 16 co-ordinates, instead of 36, but the zones of heartwood and sapwood were modelled exactly as measured, i. e., towards the stem base, the sapwood comprises up to 25 year rings, in contrast to the fixed number of ten in TREEFLEX. In the FE model, density and Young's modulus only differ between heartwood and sapwood and do not vary ring-wise. Lastly, the stem interval from 27.0 to 29.6 m was modelled in a different way: contrary to the real building of this section with finite elements, in TREEFLEX the stem ends at the position of the last stem disk at 27.0 m, and only the gravitational force exerted by the part above was added.

Simulation variants

The stem reference variant **S_Ref** is defined by the geometry and the physical and mechanical properties which represent the stem of the investigated tree as exactly as possible by the given data. The following variant descriptions only account for divergences to the reference.

Stem geometry: In variant **S_G1**, instead of the geometry of the stem at the time of felling (which was after the end of the last growing season) the geometry prior to the last growing period is considered, i. e., the last year ring is omitted. Again, the ten (and not nine) outermost year rings define the sapwood area. This variant is necessary to allow a comparison to the model which was built with the finite elements.

In **S_G2a**, the form of the stem cross section and of all year rings is represented by circles of which the areas coincide with the areas enclosed by the real year rings. In **S_G2b**, instead of a circle, the form is an oval with a constant proportion of the axes of 1:0.9 for all rings. The long axis is directed to the northwest, the proposed wind direction. The chosen oval shape resembles the shape of, at least, the lower stem disks.

In the four variants **S_G3a** – **S_G3d**, the inner stem is assumed to be more or less rotten, in the sense that it is hollow or that the affected wood no longer contributes to any mechanical stability. At breast height, the thickness of the remaining load-bearing ring is about 40%, 30%, 20% and 10% respectively, of the total radius of this stem cross section. Due to the asymmetry of the cross sections, and as only complete year rings can be included or omitted, only an approximate match of these per cent figures is possible. Modelling the stem geometry with TREEFLEX requires that the outer contour of the hollow body (lying in the stem) is always defined by the same year ring for all height positions. Therefore, if once this year ring is determined on the stem disk at breast height, the percentage of the remaining wood will change upward the stem until the hollow disappears at a certain height and the total cross section offers mechanical support.

Wood properties: In **S_WP1**, the wood density (and accordingly, the MOE) of the whole stem is uniformly decreased by 20% because one of the investigated neighbouring trees showed such reduced values. But concerning the attached branches, their density and thus, their masses were not altered. In **S_WP2**, the species-specific dependency of the density on the cambial age is substituted by the assumption that density does not differ horizontally and thus, variation in density exists only in vertical direction. In **S_WP3**, the moisture content of the entire stems was set to 100% without differentiating between heartwood and sapwood.

CROWN GEOMETRY AND PROPERTIES

On the 103 living first-order branches of the crown, the parameters length, base diameter, azimuth and inclination angle were measured (GAFFREY et al. 2001) (data on the Internet). Needle and branch dry masses were estimated branch-wise (in total, 41 kg and 68 kg, respectively), applying a randomised, bias-free sampling method (GAFFREY, SABOROWSKI 1999). It was assumed that fresh masses be twice the dry masses and the mass centroids be located mid-branch.

If further crown loads, such as snow masses, are to be considered then, in addition to the self-weight of each branch, a gravitational force due to the snow mass is added. As a reliable estimation of the vertical overlapping branches and thus, of the expected snow distribution within the crown was not possible, the snow mass on each branch was guessed as a percentage of the branch mass itself. The total snow mass the crown carries was derived by an assumed snow accumulation (kg/m^2) and by the horizontal crown projection area, which was estimated as described below.

In order to estimate sail areas, surfaces for each of the first-order branches were modelled by cubic spheroids, defined by polynomials of the third order, on the assumption of a proportionality between branch and needle mass and the volume of the spheroid. Modelling and visualisation was performed with a ray-tracing software (POV-Ray), which allows taking virtual and, if specified, undistorted, i. e., orthographic photos from any point of view (Fig. 8). The mass/volume proportionality factor, held constant for all branches, was altered until the virtual appearance of the crown coincided more or less with the crown shape of real photographs. Adjusting the virtual view in wind direction and towards the tree, the sail area of the crown was measured with the help of image analysis software.

The crown was differentiated into 17 stem sections, with regard to the positions of the main whirls. The sum of the sail areas calculated section-wise, viewed from north-west, amounts to 31 m^2 in total.

Streamlining of the crown is represented by a decreasing drag coefficient, whereas the sail area, calculated at calm, shall remain independent of wind speed. The drag coefficient c_D of the crown is set to 0.5 in the case of calm and it decreases linearly to a minimum of 0.25 at a wind speed of 20 m/s. Bending of the branches is not considered, i. e., the lengths of the acting lever arms shall not alter.

Simulation variants

The crown reference **C_Ref** represents the geometry and mass distribution of the crown according to the measured and estimated values given above.

Crown geometry: C_FEM accounts for a variant which allows nearly full comparison to the FE model. This variant is characterised by the omission of the bending moments and gravitational forces of all branches. When the finite element model was built, this step had become essential because the local application of greater gravitational forces and related moments effected a severe distortion of the finite element grid and thus, unrealistic high local stresses and strains. Though in this variant the crown mass is neglected, nevertheless, the crown sail area with corresponding wind forces is modelled (data on the Internet). Unlike the stem division in the reference, the crown was differentiated into 15 sections of equal length of one metre, with the exception of the crown tip which was not subdivided and had a length of 2.6 m.

C_G1 describes a more compact crown (Fig. 8). The volume required by the branches is reduced by 50%, but branch and needle masses were not changed. As a result, the sail area is now 25.6 m^2, which is a decrease of 18%. **C_G2** represents a partially half-sided and thus, very asymmetric crown, of which all branches up to a height of 25.0 m and oriented to the west, northwest and north are removed, simulating that a falling neighbouring tree had broken off these branches. In **C_G3**, the branch angles were substituted by ones more obtuse. The branch angles were increased step-wise from crown top (by 40°) to crown bottom (by 65°).

Snow load: The simulations of snow loads are based on an assumed snow accretion of 50 kg/m^2, which should cause a considerable stress, but not exceed the stability of the tree. With an estimation of about 15 m^2 for the horizontal crown projection, a snow mass of 750 kg, in total, be accumulated on the crown. **C_S1a**: Assuming that the branches carry snow masses proportional to the branch masses, and with 220 kg of branch fresh mass, in total, each branch shall support an additional snow mass 3.4 times its branch mass. The point of application of the snow-based gravity force is always mid-branch. In **C_S1b**, this point is shifted outwards, to a distance of two-thirds of the branch length. In **C_S2**, with respect to the real shape of the crown, it is assumed that only the branches of the light crown, above a height of 20.4 m, are covered by snow. The lower branches, reduced in length by shadowing, shall not carry an amount of snow worth mentioning. Given the same horizontal crown projection area, each branch of the light crown now supports a snow mass 4.4 times its own weight, as the fresh mass of these branches is 170 kg.

Aerodynamic properties: As aerodynamic properties of tree crowns show great variation and depend on the wind speed, **C_P1** accounts for a modified function of the drag coefficient c_D. Based on experimental data (WALSHE, FRASER 1963; MAYHEAD 1973), a parabolic decrease is described, beginning with 0.7 at calm and ending with 0.22 at a wind speed v of 33 m/s. The fitted polynomial is $c_D = 0.7093 - 0.0283v + 0.0004v^2$. In variant **C_P2**, streamlining is expressed by the reduction of the sail area instead of a decreasing drag coefficient. On the assumption that the sail area is reduced by 20% at a wind speed of 10 m/s and by 60% at 20 m/s (PELTOLA, KELLOMÄKI 1993), the parabolic interpolation $f_{red} = 1 - 0.01v - 0.001v^2$ is the reduction function which is valid in the range from 0 to 20 m/s. The drag coefficient is fixed at 0.35.

WIND CHARACTERISTICS AND WIND FORCES

Wind forces acting on the 17 differentiated crown sections are derived from hypothetical wind conditions for a north-western storm. In the absence of measured wind profiles within the stand, the potential function

$$v(z) = v_r \cdot (z/z_r)^c \qquad (3)$$

is applied, which estimates the wind speed v at any height z. It is v_r the given wind speed of 20 m/s at the reference height z_r, the height of the canopy, with z_r = 30 m. The exponent c is assumed to be 0.3 for forests (HÄCKEL 1993). (3) be valid for the wind conditions at stand edge. Dynamic effects of gustiness or tree swaying are not considered, wind speed is held constant and the tree shall deflect to a point of no return under wind loading. The wind force $F_W(z)$ acting on a sail area $A(z)$ of a crown section at height z is given by

$$F_W(z) = 0.5 \cdot \rho_a \cdot c_D \cdot A(z) \cdot v^2(z) \qquad (4)$$

The air density ρ_a is assumed to be a constant with 1.2 kg/m^3. The calculated wind forces shall be static and act horizontally and directly on the mid-sections of the stem; there is no force transmission from branch into stem and therefore, possible torsional moments due to asymmetries of the crown are neglected.

Applying a static wind loading, due to a mean wind speed averaged over a certain time period, neglects the gustiness of the wind. This can lead to a considerable underestimation of experienced forces because the short-time maximum wind speed can be three times the mean wind speed.

One possibility to take the effect of wind dynamics into account is multiplying the bending moments calculated for mean wind speed with a gust factor G, which is de-

fined as the ratio of the maximum bending moment to the mean bending moment (GARDINER et al. 1997, 2000): $G = BM_{max}/BM_{mean}$ with

$$BM_{mean} = (0.68s/h - 0.0385) + (-0.68s/h + 0.4785) \cdot (1.7239s/h + 0.0316)^{x/h}$$

$$BM_{max} = (2.7193s/h - 0.061) + (-1.273s/h + 0.9701) \cdot (1.1127s/h + 0.0311)^{x/h} \quad (5)$$

where $0.075 < s/h < 0.45$ and with s (m) the mean spacing between the trees, h (m) the mean tree height and x (m) the distance from the forest edge. Concerning the Douglas fir stand, the average tree distance was estimated to be about 8 m, resulting in $s/h \approx 0.25$ and thus, at stand edge, in a gust factor of about 2.9. Gust factor estimations that are valid inside the stand require a further multiplier given by $f_{stand} = BM_{mean}(x)/BM_{mean}(x = 0)$. With respect to the position of the analysed tree, a distance of $x = 50$ m is chosen, giving a reduced within-stand gust factor of about 1.7.

Alternatively, instead of applying a gust factor, the mean wind speed can directly be set equal to the maximum gusting wind speed, because it was shown that the extent of tree bending by gust maxima differs little from the degree of bending caused by a static wind of equal velocity (PELTOLA et al. 1993). This procedure is to be preferred in the case of simulating very high mean wind speeds as otherwise, an additional gust factor would result in unrealistic high stress values.

Simulation variants

W_Ref refers to the potential wind profile of a northwestern wind with a velocity of 20 m/s at canopy height (described above).

Wind velocity: In **W_9**, the velocity is 9 m/s. This variant is chosen in combination with snow load simulations, because this wind speed is a limit above which snow can be dislodged from the branches (PELTOLA et al. 1997). **W_0** accounts for calm.

Wind profiles: W_P1 represents the logarithmic wind profile that is commonly used in wind models (e. g., PELTOLA, KELLOMÄKI 1993; GARDINER et al. 2000). The velocity $v(z)$ at height z is estimated by

$$v(z) = v_r [\ln((z-d)/z_0)/\ln((z_r-d)/z_0)] \quad (6)$$

where v_r = 20m/s is the reference wind speed at height z_r = 30 m. Taken from literature (GARDINER et al. 2000) are the values for the roughness length z_0 (m) and the zero plane displacement d (m). As a function of stand height $z_0 = 0.06 \cdot h$, the roughness parameter here is 1.8 m. Outside the stand, the zero plane displacement can normally be neglected (PELTOLA, KELLOMÄKI 1993) and thus, $d = 0$.

W_P2 describes an empirical, within-stand wind profile

$$v(z) = v_r \cdot [1 + \alpha(1 - z/z_r)]^{-2} \quad (7)$$

proposed by LANDSBERG and JAMES (1971) for a Sitka spruce stand. The parameter α is extremely influenced by the leaf-area density. But in the absence of such data, e. g., the refined approach of LANDSBERG and JARVIS (1973) which accounts for this dependency could not be applied and thus, the constancy $\alpha = 2.5$, proposed in the first-mentioned publication, was applied.

MODELLING ELASTOMECHANICS OF THE TREE

The central key for prognosticating stress and strain of the wood fibres in the stem for a given loading case is the calculation of the elastic curve of the stem axis. It is only the stable state of the bent tree, at standstill, which is of interest, when acting external forces and bending moments are in equilibrium with counteracting internal ones. External bending moments result from wind forces and from gravity of tree masses (stem, branch, needle and possibly snow and ice masses) that are not symmetrical relative to a perpendicular axis going through the foot of the tree. The internal bending moments depend on area and form of the stem cross sections, the elastic properties of the wood and the degree of the curvature of the tree. With the differential equation system set up, finding the steady state will require an iterative solution, because any displacement of the tree and its masses will change the acting forces which, again, influence the displacement themselves.

Common basic assumptions and their adoption in the model

Usually, according to the theory of classic elastomechanics, the stem of a tree is considered to behave as a beam (TIMOSHENKO 2000; SZABÓ 2001). It is to be proven whether the underlying assumptions in such a case actually hold true.

(i) If the ratio of length to diameter of a beam is great (> 20 : BAUMANN 1922; > 25 : SZABÓ 2001) transverse forces (shear) can be neglected. An initially even cross section will remain even and perpendicular to the bent stem axis.
For most trees, due to their slenderness, this is valid. Therefore, the strain of the fibres is proportional to the distance from the neutral axis. The neutral axis, related to a distinct cross section, is defined by the line of zero strain.

(ii) The deformation of the wood follows a linear-elastic pattern described by HOOKE's law; i. e., the modulus of elasticity E determines the relation between strain ε, the relative change in length $\Delta l / l$, and stress σ : $\sigma = E \cdot \varepsilon$. The elastic properties of the beam are homogeneous. The existence of such a linear-elastic interval is generally accepted, though it is uncertain to indicate where the transition zone of plastic deformation begins. (Here, this aspect must be left aside, too.) Homogeneity of material and thus, of mechanical properties just does not exist. This simplification might only serve for a first, rough approach but does not do justice to the observed spatial variation in MOE.

(iii) The unloaded beam is not curved; its straight axis is given by the line which intersects the mass centroids of all cross sections. All external forces act perpendicularly on the axis of the stem and lie within a vertical plane, the force or momentum plane, which includes the tree axis.

In approximation, without loading of the tree, the axis of most stems may be straight, and therefore, this assumption is adapted here, too. But instead of mass centres, the centroids are derived by weighing with the bending stiffness of the year rings. As for the acting forces, due to non-homogeneous air flow and an asymmetric crown, normally they do not lie within a plane and moreover, do not run through the stem axis. Additional torsional moments are the consequence.

In the present state of TREEFLEX, torsional moments are still ignored. But TREEFLEX has no restrictions concerning the acting force system and thus, as a full 3-D model, the spatial curvature of the axis can be represented completely.

Stress and strain for a stem with irregular cross-sections and varying MOE

The stem of a tree is considered to be a perpendicular cantilever which is firmly clamped (stiff anchorage) at its foot, where the origin of a Cartesian co-ordinate system shall lie (Fig. 1). As stem analyses reveal, the form of the stem cross sections and of the inner year rings is rarely found to be circular or oval, but it can be extremely irregular (Fig. 2). Furthermore, contrary to artificial materials, the mechanical properties of wood show no constancy

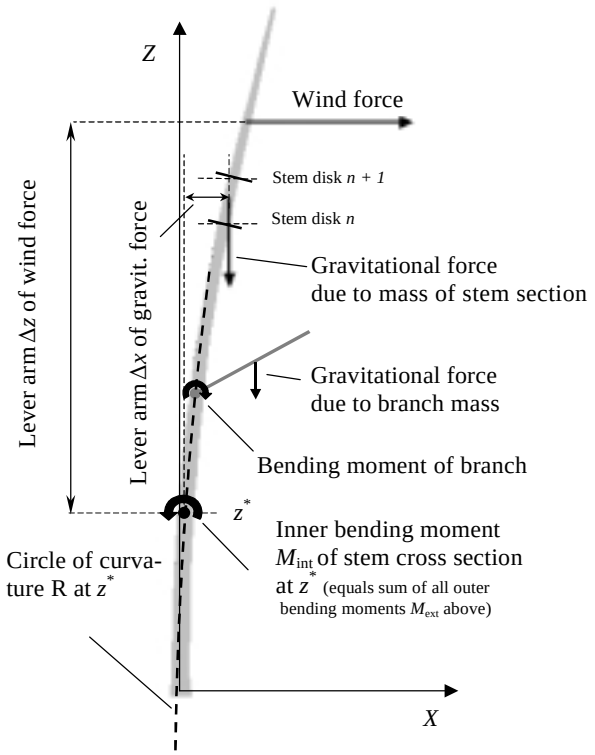

Fig. 1. Acting forces and bending moments for a tree subjected to wind loads and self-weight

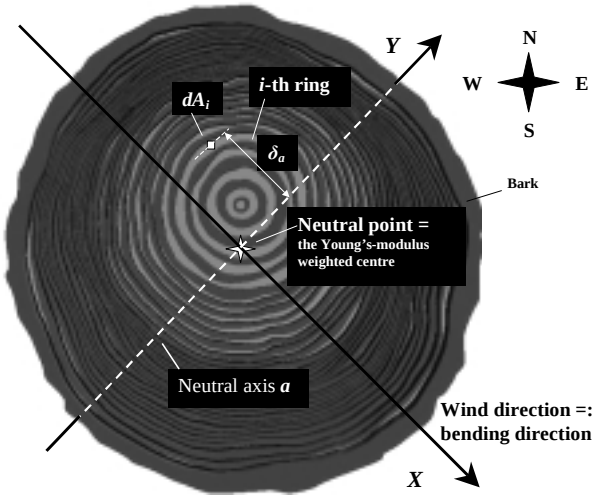

Fig. 2. Stem disk of Douglas fir No. 104 at a height of 0.40 m, considered to be a composite with ring-specific material properties; location of neutral axis and neutral point according to given bending direction (year rings alternating in light and dark grey)

but vary spatially within a stem. In the model, it is assumed that each year ring differs in the MOE, but within a ring, the elasticity shall be constant. Thus, the wood of the stem is modelled as a composite (WAINWRIGHT et al. 1976; SPECK et al. 1990, 1996; VINCENT 1990) which consists of n layers with specific Young's moduli E_i, $i = 1,...,n$. (The vertical variation is also taken into account according to the disk-specific differences, but for simplification of the formulae, corresponding indices are omitted.)

In the case of an irregular shape of the cross section, the bending direction is of great importance. Referring to a distinct cross section (Fig. 2), a local co-ordinate system is chosen with the x-axis in bending direction and the origin in the neutral point, which is the Young's-modulus weighted centre. Then, the y-axis coincides with the neutral axis a, and δ_a is the distance to a infinitesimal area dA_i located in the i-th year ring, which has the area A_i. With respect to the location of the neutral axis, the axial second moment of area I_a of the total cross-sectional area A is the sum of all ring-specific contributions $I_{a,i}$.

$$I_a = \sum_{i=1}^{n} I_{a,i} = \sum_{i=1}^{n} \int_{A_i} dA_i \cdot \delta_a^2 \qquad (\mathrm{m}^4) \qquad (8)$$

In combination with the MOE, the product $S = E \cdot I$ (Nm^2) is the flexural stiffness (bending stiffness) which characterises the resistance of the stem against bending (at a certain height). As the Young's modulus E_i is ring-specific, the elasticity of the total cross section, denoted as the "structural" Young's modulus $E_{\mathrm{st},a}$ (SPECK et al. 1996), is given by

$$E_{\mathrm{st},a} = \sum_{i=1}^{n} E_i \cdot \frac{I_{a,i}}{I_a} \qquad (9)$$

and thus, the flexural stiffness

$$S_a = \sum_{i=1}^{n} S_{a,i} = \sum_{i=1}^{n} E_i \cdot I_{a,i}$$

At the state of equilibrium between the sum of all acting external bending moments and the counteracting inner ones, $M_{ext,\,a} \equiv M_{int,\,a}$, the curvature $1/R$ of the stem axis (Fig. 1) is

$$\frac{1}{R} = \frac{M_{ext,a}}{E_{st,a} \cdot I_a} \tag{10}$$

As the stress $\sigma_i(\delta_a)$ in the i-th year ring at a distance δ_a from the neutral axis a is given by $\sigma_i(\delta_a) = E_i \cdot \delta_a / R$, and inserting (9) and (10), it is

$$\sigma_i(\delta_a) = \frac{E_i \cdot M_{ext,a} \cdot \delta_a}{\sum_{i=1}^{n} E_i \cdot I_{a,i}} \tag{11}$$

Applying HOOKE's law, the corresponding strain is

$$\varepsilon_i(\delta_a) = \frac{\sigma_i(\delta_a)}{E_i} = \frac{M_{ext,a} \cdot \delta_a}{S_a} \tag{12}$$

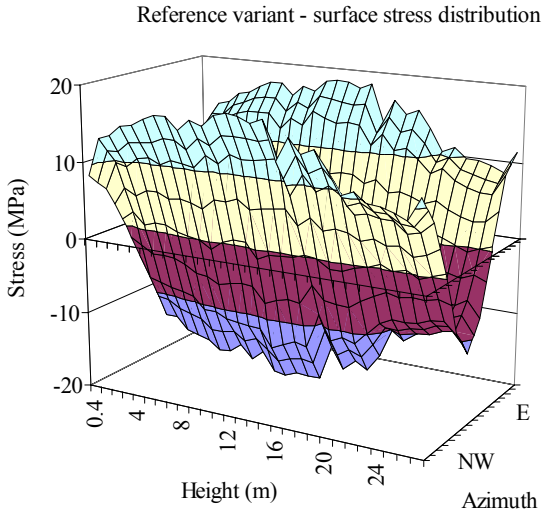

Fig. 3a. Surface stress distribution calculated for the reference variant defined by the original stem geometry and mechanical properties (S_Ref), the original crown geometry and mass distribution (C_Ref), and a north-western wind with a velocity of 20 m/s and a potential wind profile (W_Ref)

which illustrates that the strain in a specific year ring does not depend on its local, ring-specific elastic property but on the flexural stiffness of the total cross section. As usually maximum stress and strain at the periphery of the stem, experienced in the n-th year ring, are of interest, the maximum distance $\delta_{max,\,a}$ to the neutral axis is to be chosen.

A complete description of the differential equation approach and its solution is given in the Appendix.

Technical details of modelling

At present state, the TREEFLEX simulation software consists of two, non-integrated modules. A conventional database stores measured geometry and material properties data and calculates and exports, by Visual Basic® scripts, the complete data sets. These data are required by the second module (developed by the authors), which iteratively solves the differential equation problem for a given loading case. Output data are stress and strain at the stem surface and the displacement of the stem axis. Graphical visualisation with optional DXF and POVRay export is possible.

RESULTS

Each simulation of the elasto-mechanical bending of the tree is based on the characteristics, which are given in the chosen variant combinations for stem, crown and wind properties (Table 1). Calculated are the stress values at stem periphery (excluding bark) and at the heights of all stem disks. With respect to the wind direction, only data of the fibres oriented to north-west are presented because they experience the highest tensile stresses.

STRESS DISTRIBUTION OF THE REFERENCE VARIANT

The 3-D grid in Figure 3a, which presents the stress distribution at the stem surface, does not at all indicate

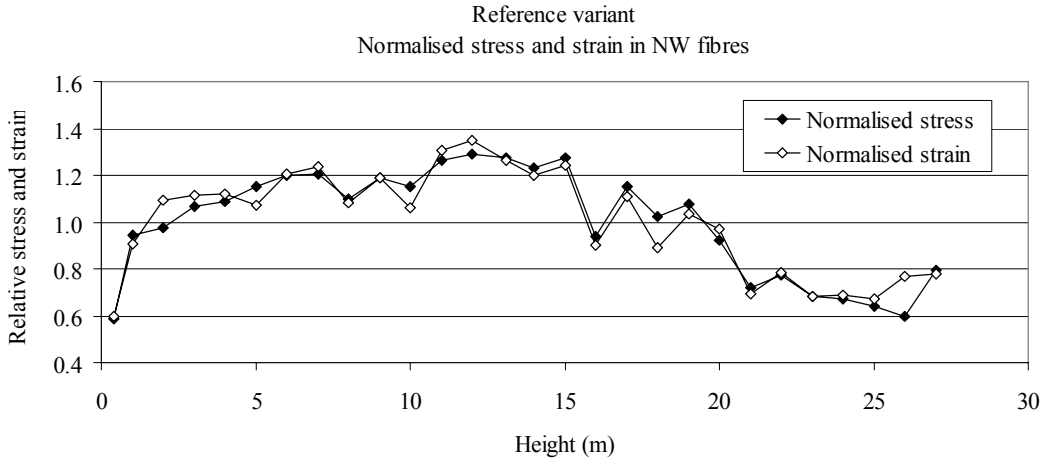

Fig. 3b. Normalised stress and strain for the reference variant (S_Ref + C_Ref + W_Ref)

Table 1. Results of the tree-bending simulations

Model variant combinations			Height (m)																										
Stem	Crown	Wind	0.4	1.3	2.0	3.0	4.0	5.0	6.0	7.0	8.0	9.0	10.0	11.0	12.0	13.1	14.0	15.0	16.0	17.0	18.0	19.0	20.0	21.0	22.0	23.0	24.0	25.0	26.0	27.0
			Tensile stresses in surface fibres oriented to NW (or NNW*) (MPa)																										
TREEFLEX																													
Reference variant																													
S_Ref	C_Ref	W_Ref	8.4	13.5	14.0	15.3	15.6	16.5	17.2	17.3	15.8	17.1	16.6	18.1	18.5	18.3	17.7	18.3	13.5	16.5	14.7	15.5	13.2	10.3	11.1	9.8	9.7	9.2	8.5	11.4
Stem geometry variants																													
S_G1	C_FEM	W_Ref*	6.1	9.8	9.9	11.0	11.3	11.7	12.0	12.0	10.6	11.5	11.0	12.3	11.9	11.7	11.3	11.4	8.5	10.2	8.5	8.9	7.7	6.2	7.5	7.3	7.8	7.5	8.0	16.1
S_G2a	C_Ref	W_Ref	9.0	14.8	15.0	16.7	17.2	18.0	18.7	18.1	16.6	18.4	17.6	19.9	19.7	19.7	19.0	19.4	14.6	17.7	15.5	16.6	13.9	10.9	11.8	10.3	10.1	9.3	8.7	11.6
S_G2b	C_Ref	W_Ref	8.2	13.4	13.6	15.2	15.6	16.3	16.9	16.4	15.0	16.6	15.8	18.0	17.8	17.8	17.2	17.5	13.2	15.9	14.0	15.0	12.6	9.9	10.6	9.3	9.2	8.5	8.0	10.7
S_G3a	C_Ref	W_Ref	10.5	16.9	16.9	18.2	18.3	18.5	19.2	19.3	17.4	19.1	17.8	19.0	18.9	18.6	18.0	18.6	13.7	16.8	14.9	15.7	13.4	10.5	11.2	9.9	9.8	9.3	8.6	11.4
S_G3b	C_Ref	W_Ref	12.7	20.4	20.1	21.6	21.7	21.6	22.4	22.3	20.2	23.2	21.7	22.6	21.7	21.1	20.3	20.2	14.9	17.6	15.5	16.2	13.9	10.8	11.6	10.2	10.0	9.5	8.7	11.5
S_G3c	C_Ref	W_Ref	17.2	27.7	26.8	29.2	30.2	30.2	30.1	29.2	26.1	30.7	29.2	30.5	29.2	28.7	27.8	28.2	21.4	23.9	20.2	19.8	16.2	12.1	12.6	11.0	10.7	10.0	9.0	11.8
S_G3d	C_Ref	W_Ref	30.9	49.6	49.8	53.0	55.6	52.9	52.5	49.9	44.1	55.7	53.8	54.9	53.3	54.3	51.6	54.0	42.6	47.9	42.2	41.6	31.9	23.9	20.7	15.9	13.3	11.6	9.6	11.9
Stem wood property variants																													
S_WP1	C_Ref	W_Ref	8.7	14.0	14.6	15.9	16.2	17.2	18.0	18.0	16.5	17.9	17.3	19.0	19.4	19.2	18.6	19.2	14.2	17.4	15.5	16.4	14.0	11.0	11.8	10.4	10.2	9.7	8.8	11.7
S_WP2	C_Ref	W_Ref	8.2	13.2	13.7	15.0	15.3	16.3	16.9	16.9	15.5	16.7	16.2	17.7	18.1	18.0	17.4	17.9	13.2	16.3	14.5	15.2	13.0	10.1	10.8	9.6	9.5	9.1	8.6	11.5
S_WP3	C_Ref	W_Ref	8.4	13.6	14.1	15.4	15.7	16.7	17.4	17.3	15.9	17.1	16.6	18.1	18.5	18.3	17.6	18.2	13.3	16.4	14.6	15.3	13.0	10.2	10.9	9.6	9.5	9.1	8.6	11.5
Crown geometry variants																													
S_Ref	C_G1	W_Ref	7.0	11.2	11.6	12.7	12.9	13.7	14.3	14.3	13.1	14.2	13.8	15.1	15.4	15.3	14.8	15.3	11.3	13.9	12.4	13.1	11.2	8.8	9.3	8.2	8.1	7.7	7.1	8.7
S_Ref	C_G2	W_Ref	8.7	14.1	14.6	16.0	16.4	17.4	18.2	18.3	16.8	18.3	17.7	19.5	20.1	20.1	19.6	20.5	15.2	19.0	17.2	18.6	16.2	13.0	13.7	12.1	11.1	9.6	8.7	11.6
S_Ref	C_G3	W_Ref	8.5	13.6	14.1	15.4	15.7	16.6	17.3	17.3	15.8	17.1	16.6	18.1	18.4	18.2	17.6	18.1	13.3	16.3	14.4	15.1	12.9	9.9	10.9	9.9	9.9	9.4	8.7	11.1
Crown snow load variants																													
S_Ref	C_S1a	W_0	1.1	2.1	2.0	2.3	2.2	2.0	2.7	2.5	2.8	3.6	3.7	4.1	4.6	5.1	5.0	5.6	3.9	5.6	5.7	7.0	5.0	3.7	0.8	-1.1	-0.5	0.8	3.1	2.7
S_Ref	C_S1a, C_G3	W_0	0.4	0.9	0.8	1.0	0.9	0.7	1.1	1.0	1.2	1.6	1.6	1.8	2.1	2.3	2.3	2.5	1.7	2.5	2.7	3.4	2.0	1.0	-2.3	-4.9	-4.2	-1.7	2.1	1.5
S_Ref	C_S1a	W_9	8.6	14.1	15.3	17.1	17.7	19.0	20.4	20.8	19.7	22.2	21.7	24.7	26.0	26.8	26.8	29.0	21.1	27.8	25.6	28.8	24.7	19.0	18.4	15.1	14.7	14.9	14.7	17.4
S_Ref	C_S1b	W_9	9.6	15.6	17.0	19.1	19.8	21.1	22.8	23.2	22.0	24.9	24.3	27.8	29.3	30.3	30.4	33.1	24.0	32.0	29.5	33.6	28.8	22.3	21.5	17.6	17.3	17.7	17.5	19.8
S_Ref	C_S2	W_0	1.3	2.6	2.5	2.8	2.7	2.4	3.3	3.0	3.4	4.3	4.4	5.0	5.5	6.1	6.0	6.7	4.6	6.9	6.7	8.2	6.5	5.3	1.9	-0.4	0.5	1.9	4.5	4.1
Wind and crown aerodynamic property variants																													
S_Ref	C_Ref	W_9	2.5	4.0	4.2	4.6	4.7	5.0	5.2	5.2	4.8	5.2	5.0	5.5	5.7	5.6	5.5	5.7	4.2	5.2	4.7	5.1	4.3	3.3	3.1	2.4	2.5	2.7	2.9	3.8
S_Ref	C_Ref	W_P1	7.9	12.7	13.2	14.5	14.7	15.6	16.3	16.3	14.9	16.2	15.7	17.2	17.5	17.4	16.8	17.4	12.8	15.8	14.1	14.9	12.8	10.0	10.7	9.5	9.4	9.0	8.4	11.3
S_Ref	C_P1	W_Ref	10.1	16.2	16.8	18.3	18.7	19.7	20.6	20.6	18.8	20.4	19.7	21.6	22.0	21.8	21.1	21.7	16.0	19.6	17.4	18.3	15.7	12.3	13.3	11.9	11.6	11.0	10.0	13.4
S_Ref	C_P2	W_P1	5.2	8.3	8.6	9.5	9.6	10.2	10.7	10.7	9.8	10.6	10.2	11.2	11.5	11.4	11.0	11.4	8.4	10.3	9.2	9.7	8.2	6.4	6.6	5.6	5.5	5.4	5.3	6.9
S_Ref	C_P1	W_P2	2.7	4.3	4.5	4.9	5.0	5.3	5.6	5.6	5.2	5.6	5.5	6.1	6.3	6.3	6.2	6.5	4.9	6.2	5.7	6.3	5.6	4.5	4.8	4.3	4.8	5.1	5.6	8.1
Finite element model																													
S_FEM	C_FEM	W_Ref*	4.5	10.1	8.0	10.2	10.6	10.4	11.6	11.5	8.9	10.6	9.9	12.0	10.3	12.6	10.8	11.3	8.0	10.2	7.9	8.8	7.9	5.9	7.9	7.9	8.5	8.5	9.5	25.3

Explanations of the abbreviations are given in the chapter “Simulation variants”

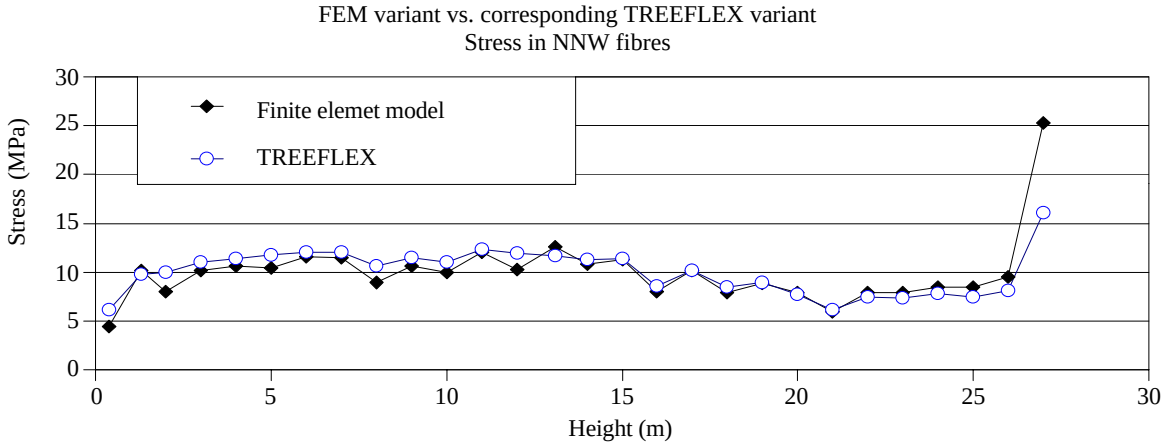

Fig. 4. Comparison between variants modelled with finite elements (S_FEM + C_FEM + W_Ref) and with TREEFLEX (S_G1 + C_FEM + W_Ref), stresses presented for the outer fibres oriented to NNW

uniformity: regarding a fixed azimuth orientation, here NW, where stresses are maximum, the values are relatively small near the base of the stem (8 MPa), increase within the branch-free part of the bole (17–18 MPa), and decrease within the crown (8–9 MPa), but with a distinct rise in the uppermost part. Single major deviations, e. g., at the height of 16 m (13.5 MPa), find their explanation in local stem thickenings. The data rows of stress and strain can be best compared if they are normalised by the mean values (Fig. 3b). The curves are very similar; some distinct deviations are caused by a significant, locally increased or decreased wood density (mean density: 0.55 g/cm^3, maximum density: 0.65 g/cm^3 at 19 m, minimum density: 0.44 g/cm^3 at 26 m).

FINITE ELEMENT MODEL VS. HOLISTIC APPROACH OF TREEFLEX

The stress values for both, the FEM simulation (S_FEM, C_FEM, W_Ref) and the TREEFLEX calculations (S_G1, C_FEM, W_Ref) differ significantly from those of the reference variant, though, in principal, the vertical stress distribution pattern is quite similar (Table 1). Calling to mind that the crown mass is neglected in these variants and that not the maximum stresses in the northwest-oriented fibres were estimated, but stresses in NNW direction, thus, two reasons for the generally lower values are given. At first sight, the much higher values in the upper crown at a height of 27 m could be astounding. But in C_FEM and S_G1, the stem contour is defined by the

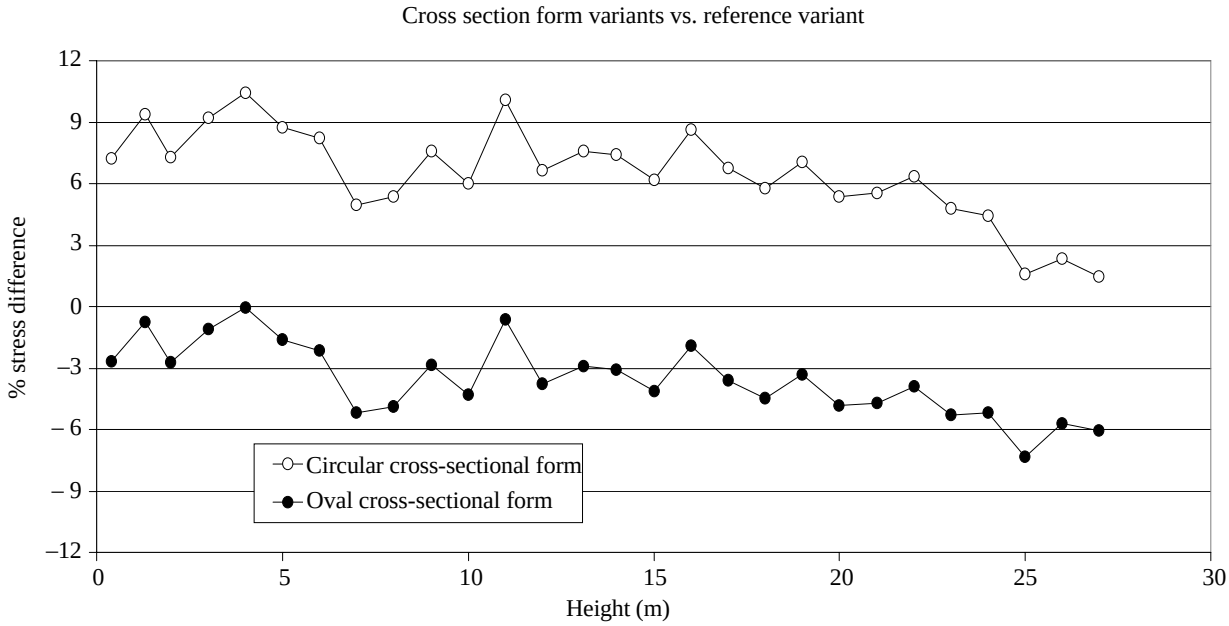

Fig. 5. Influence of the form of the stem cross section on experienced stresses, variants S_G2a (circular form) and S_G2b (oval form), combined with C_Ref + W_Ref

second-to-last year ring. Compared to the contour in C_Ref, it is this "missing" last year ring which essentially contributes to the lack of bending stiffness of the very thin stem of the crown tip.

Fig. 4 shows the results of the finite element model and the holistic approach, i. e., the calculated stress values for the outer fibres oriented to north-northwest. Though, with the exception of the crown tip, the stress profiles match each other quite well, the (absolute) stress values of the finite element model are lower in the branchless part of the stem, with increasing divergence towards the foot and attain –15% (averaged for the lowest three heights). Probably, the deviation in modelling heart- and sapwood zones and thus, different gravity forces due to the inner mass distribution of the stem are, to some extent, responsible. In contrast, at a height of 27 m, the finite element model predict a more than 55% higher stress. This might be explained by the different way of how the models represent the last stem segment and the corresponding gravitational forces.

EFFECT OF STEM GEOMETRY

Unlike reality, stem cross sections are mostly modelled as circles and very rarely as ovals. As shown in Fig. 5, substituting the most irregularly formed base stem disks by circular ones can induce stresses that are 10% higher. Towards the top, these differences diminish because there the reaction wood formation had not yet been so significant and thus, the cross sections show less ovality. Correspondingly, oval cross sections modelled and oriented in order to approximately coincide with the form of the base disk result in equal or slightly reduced stresses at the stem base, but in increasing stress underestimation towards the top of the tree (–6%).

Of great importance is the simulation of partially rotten stems because it is often a decision of public safety whether such trees are to be removed, or not. Assuming a circular cross-section, a limitation of the supporting area to an outer ring, which has a remaining wall thickness of 40%, 30%, 20% or 10%, will result in an area reduction of 36%, 49%, 64% and 81%, and in a reduction in the axial second moment of area I (and bending stiffness S, too, if the area has a homogeneous MOE distribution) of 13%, 24%, 41% and 65.6%. These theoretical figures are approximately verified (Fig. 6a–6c) when regarding the real cross sections and the calculated bending stiffness with respect to the neutral axis, i. e., here, with respect to the assumed south-eastern bending direction. It is found that these weakened stems will experience a stress increase of up to about 25%, 50%, 100% and over 250% at the stem base (Fig. 6d) if they do not break before, which is expected to happen in the last case, because the absolute stress values of about 55 MPa exceeds the strength limit (Table 1).

EFFECT OF WOOD PROPERTIES

A general reduction of 20% of the wood density (and MOE) results in a stress increase from 4% (bottom) to 6% (mid-crown), and then, falling off, to 2% (top) (Fig. 7). The

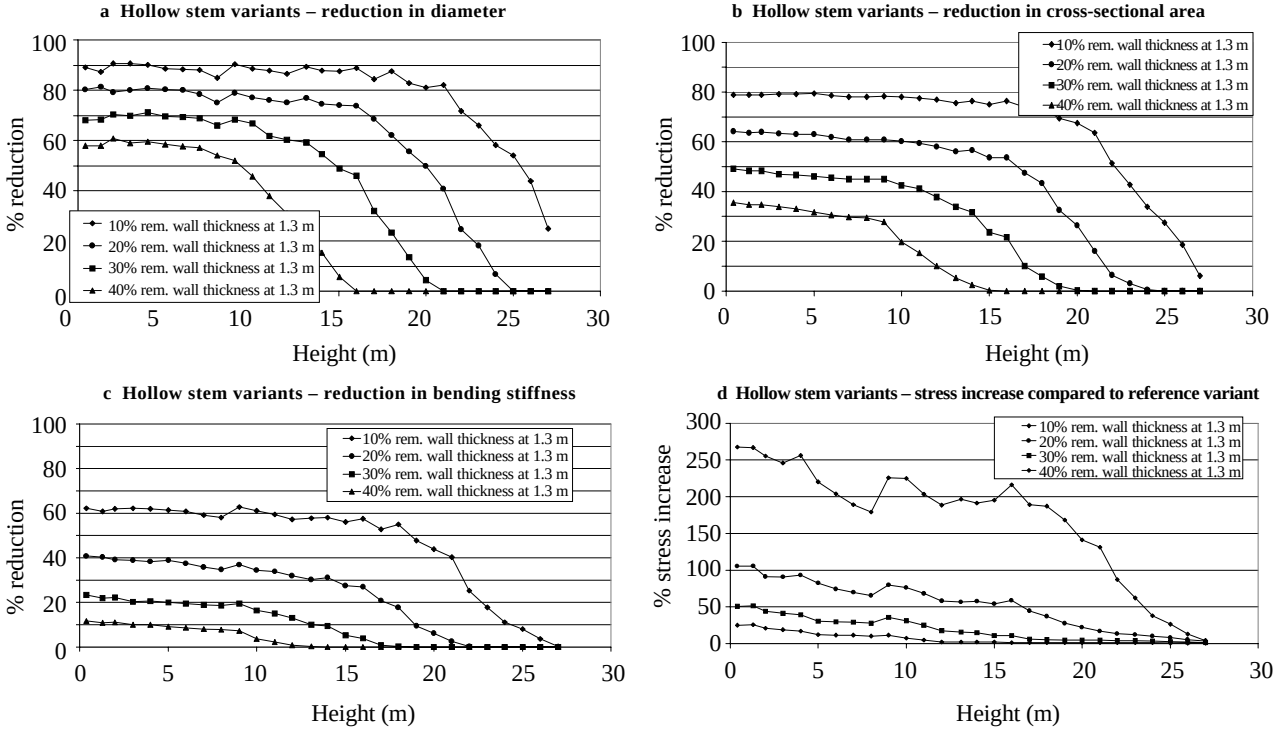

Fig. 6a. Hollow stem variants (S_G3a–S_G3d, combined with C_Ref + W_Ref) – reduction in diameter
Fig. 6b. Hollow stem variants (S_G3a–S_G3d, combined with C_Ref + W_Ref) – reduction in cross-sectional area
Fig. 6c. Hollow stem variants (S_G3a–S_G3d, combined with C_Ref + W_Ref) – reduction in bending stiffness
Fig. 6d. Hollow stem variants (S_G3a–S_G3d, combined with C_Ref + W_Ref) – stress increase compared to reference variant

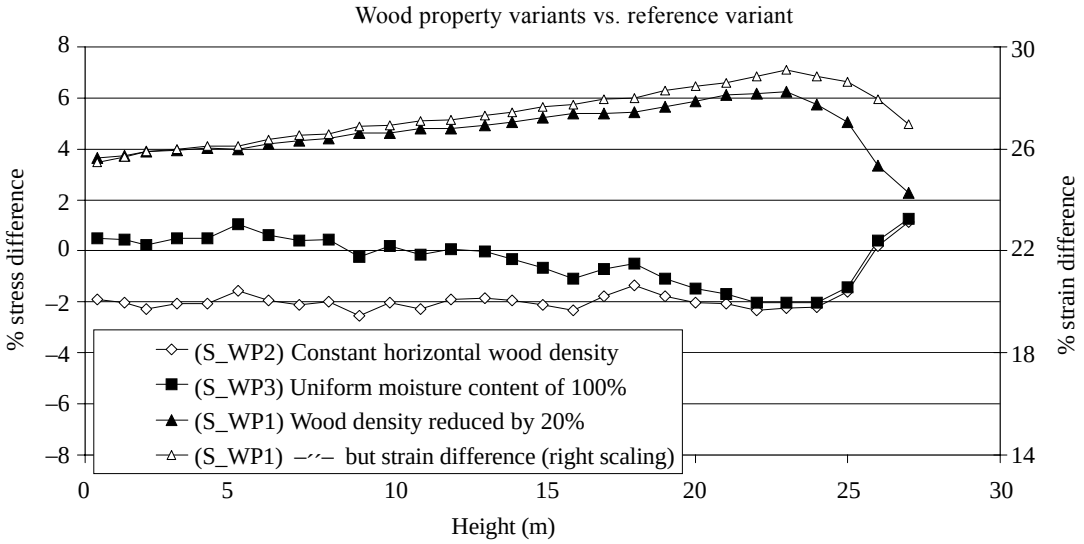

Fig. 7. Influence of wood properties on experienced stresses, variants S_WP1, S_WP2 and S_WP3 in comparison to reference S_Ref, combined with C_Ref + W_Ref

strain difference which follows an identical pattern is much higher because of the high deflection of the less rigid stem: it ranges from 25 to 29%. In contrast, in both other simulated wood-property variants, the magnitude of stress and strain differences are quite similar. A constant moisture content of 100% which slightly increases the stem mass in total effects relatively little, especially in the lower half of the stem. There are maximum changes between + 1% and –2% . In the case of a uniform horizontal density and MOE distribution, the stresses decrease by 2%, with the exception of the uppermost stem part, where a minimal increase can be found.

Fig. 8. Crown variants visualised with POV-Ray, view from NW. From left to right: reference, 50% volume reduction (C_G1), half-sided crown (C_G2) and obtuse branch angles (C_G3)

EFFECT OF CROWN PROPERTIES

A crown volume reduction of 50 % is accompanied by, on average, 18% decreased sail area (Figs. 8, 9, calculated by image analysis). As this variable directly affects the experienced wind forces, the stress reduction ranges between 15 and 24%. Less significant, if at all, is the effect of changing the branch angles, here, by substituting the original by obtuse ones. But very remarkable is the reaction of the highly asymmetric crown. The one-sided removing of branches results mid-crown in a maximum stress increase of 25%.

EFFECT OF SNOW MASSES

If the masses of a snow fall of 50 kg/m^2 are distributed over the crown equally, i. e., each branch carrying a snow load proportional to its self-weight (variant C_S1a), then, already in calm, stresses up to 7 MPa are possible (Fig. 10a). The common centre of tree and snow masses lies outside the tree axis and is oriented to south-south-east. Thus, the stem is supposed to be bent in this direction in the absence of wind. As stresses are calculated for the northwest and not for the north-northwest direction, these values do not represent the sustained maximum stresses which are (slightly) higher.

A peculiarity of this tree is a significant local crown mass eccentricity in the interval from 23 to 25 m due to missing southward-oriented branches. This causes a stress minimum, even with negative, i. e., compressive stresses at the north-west side of the stem. Unlike the case where wind forces dominate, at calm, obtuse branch angles significantly reduce stresses below a height of 20 m by 50 to 60%. Otherwise, the stress reversal in the mentioned asymmetric crown segment is enhanced because, in this variant, the branches stand away nearly horizontally (Fig. 8). Lastly, if

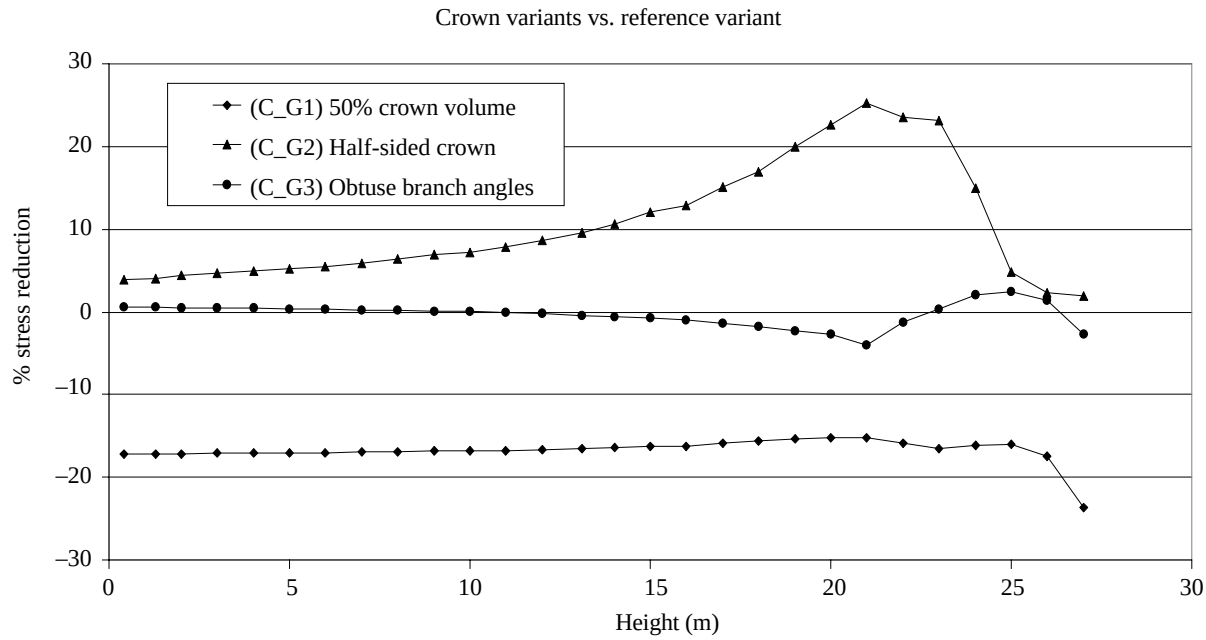

Fig. 9. Influence of crown geometry on experienced stresses, variants C_G1, C_G2 and C_G3 compared to C_Ref, combined with S_Ref + W_Ref

the snow settles down only on the light crown, stresses in the main part of the stem are increased by 20%.

If wind is brought into play, at a wind speed of 9 m/s the contribution of the experienced stresses explained by the snow masses is between 70 and 80% (Fig. 10b), and total stress values of nearly 30 MPa are possible. Shifting the assumed snow mass centroids from mid-branch outwards (C_S2) enforces the stress by 11 to 19%.

EFFECT OF WIND PROFILES AND AERODYNAMIC CROWN PROPERTIES

Relatively little changes, when instead of the potential wind profile (W_Ref) a logarithmic one (W_P1) is applied (Fig. 11a): the slightly reduced wind speed coincides with a stress difference of about 5% in the lower part of the stem. Much more influence is exerted by modifications of

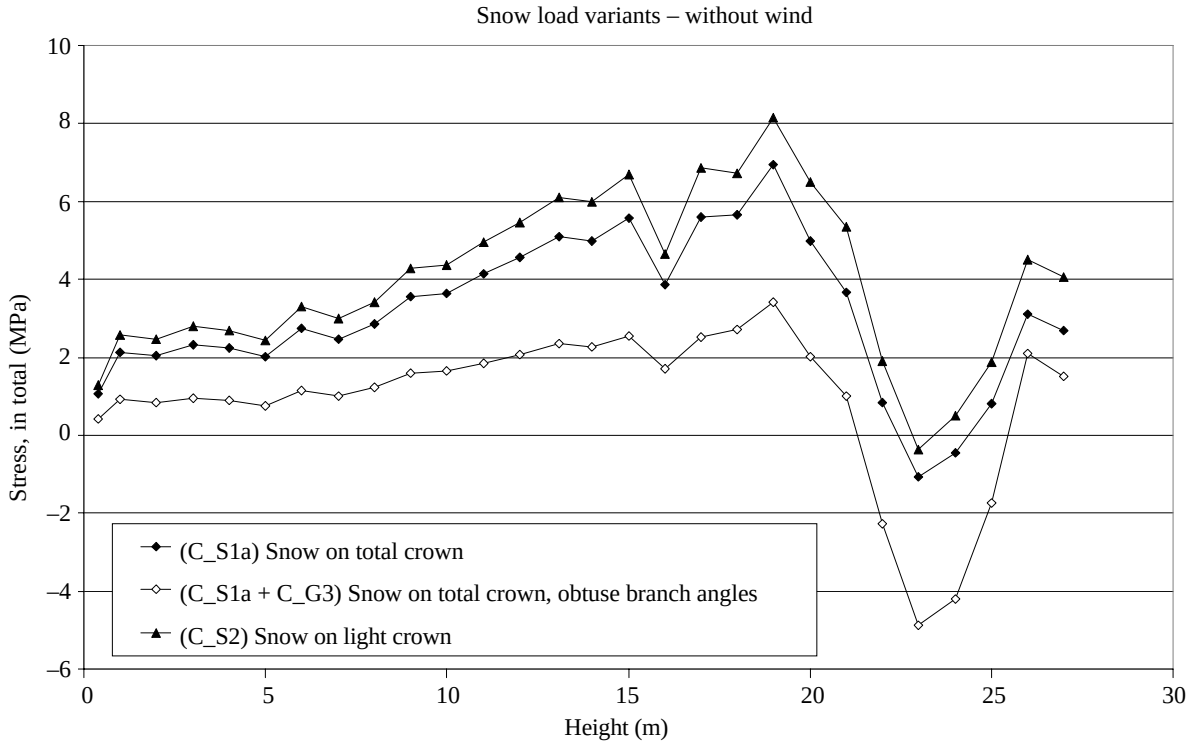

Fig. 10a. Effect of snow masses and their distribution (C_S1a, C_S2), and of branch angles (C_G3), without wind (W_0), combined with stem properties of the reference (S_Ref)

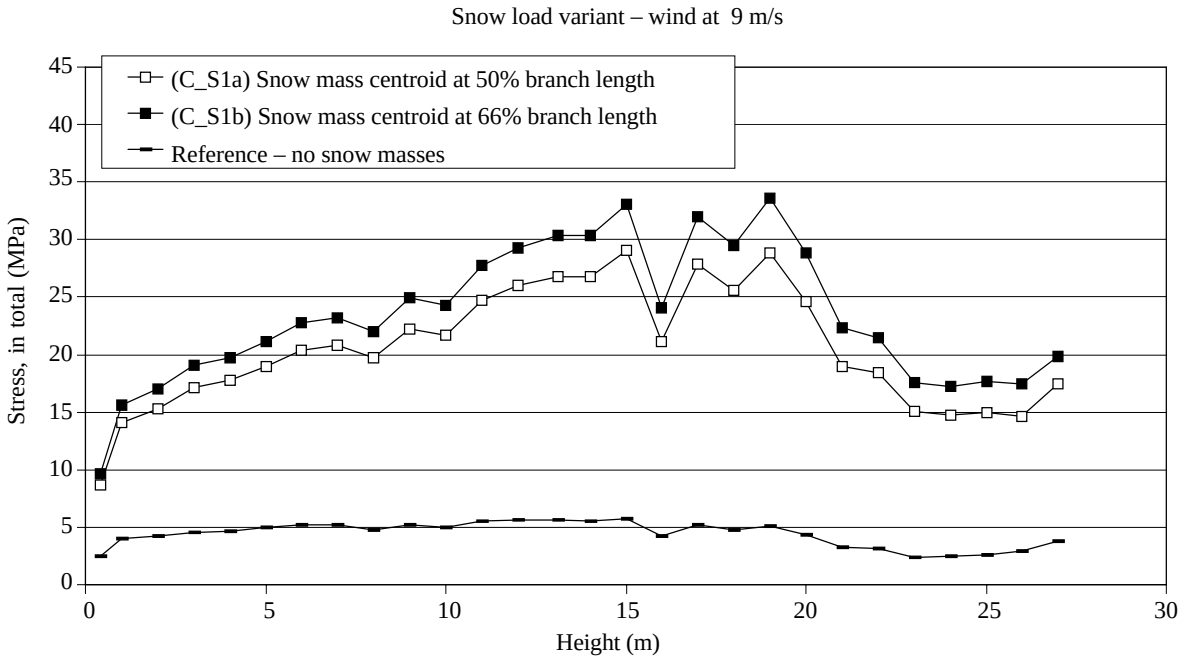

Fig. 10b. Effect of snow masses and their distribution (C_S1a, C_S1b), with wind (W_9), combined with stem properties of the reference (S_Ref)

the drag coefficient (C_P1) or of the streamlined sailing area (C_P2). The same magnitude of increase (about 20%) and decrease (about 40%) respectively, of these parameters, on average, is reflected in the change of stresses along the stem. In contrast, applying a quite different within-stand wind profile (W_P2) results in a diverging stress pattern. Besides remarkably reduced stresses of 67% on average because of the lower wind velocity inside the stand, the normalised stresses are higher in the crown section; namely the uppermost values are striking (Fig. 11b).

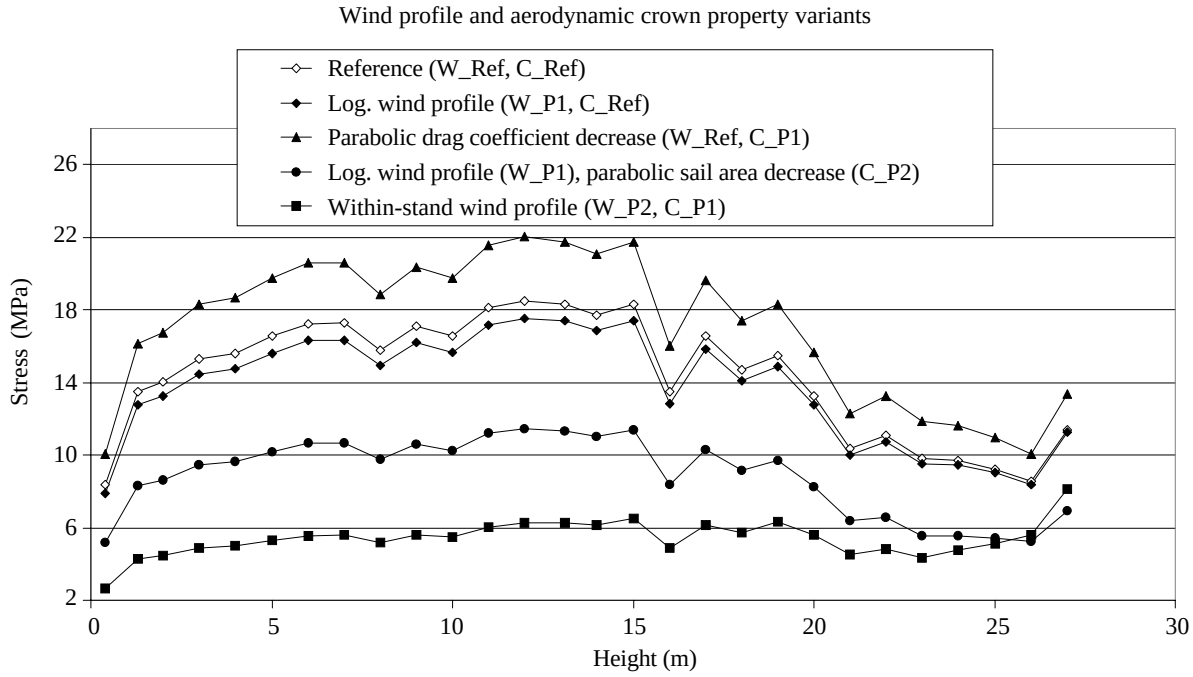

Fig. 11a. Effect of wind profiles (W_Ref, W_P1, W_P2) and aerodynamic crown properties (C_P1, C_P2), combined with stem properties of the reference (S_Ref)

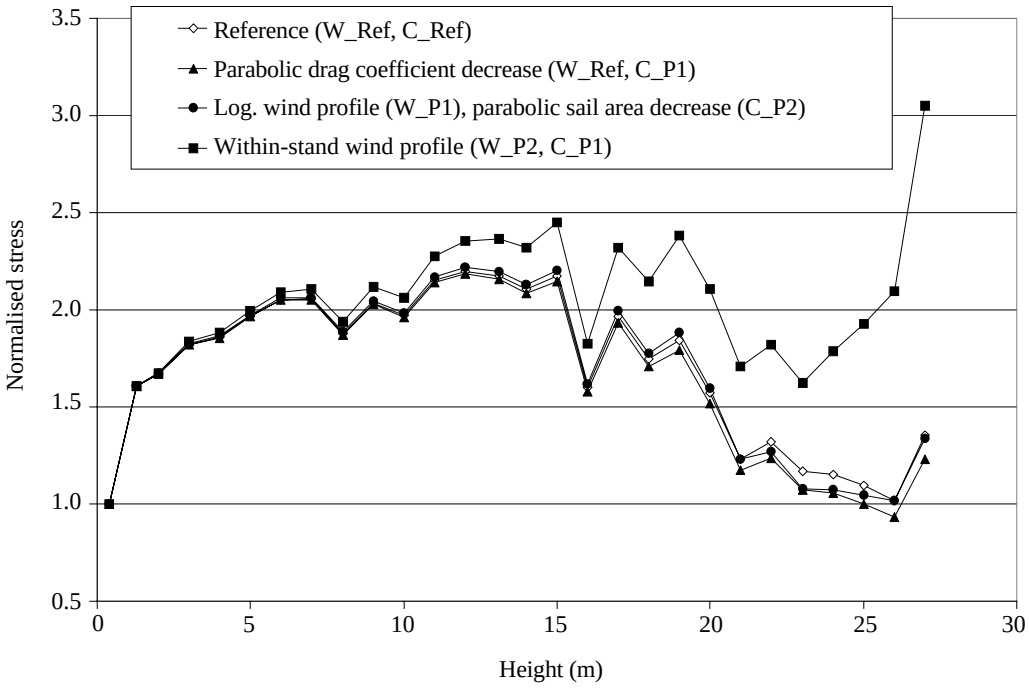

Fig. 11b. Effect of wind profiles and aerodynamic crown properties: normalised stresses by values at height 0.4

SAFETY AGAINST FRACTURE FAILURE

Inverse to the stress and strain curves (Fig. 3a,b) are the curves which demonstrate the relative safety against fracture failure (Fig. 12). Safety is defined as the ratio between breaking strength (modulus of rupture, MOR) and sustained stress or between strain at the proportional limit, where irreversible plastic deformation begins, and the sustained strain. As the focus is on the living tree, the strength of the fresh wood of the stem is of interest. Unfortunately, such measurements are rarely performed on complete, green stems (FONS, PONG 1957) but mostly on ideal specimen of green wood (U.S.D.A. Forest Products Laboratory 1989; WESSOLLY, ERB 1998). Therefore, to account for the weakening influence of structural inhomogeneities in the stem, the bending strength of the total

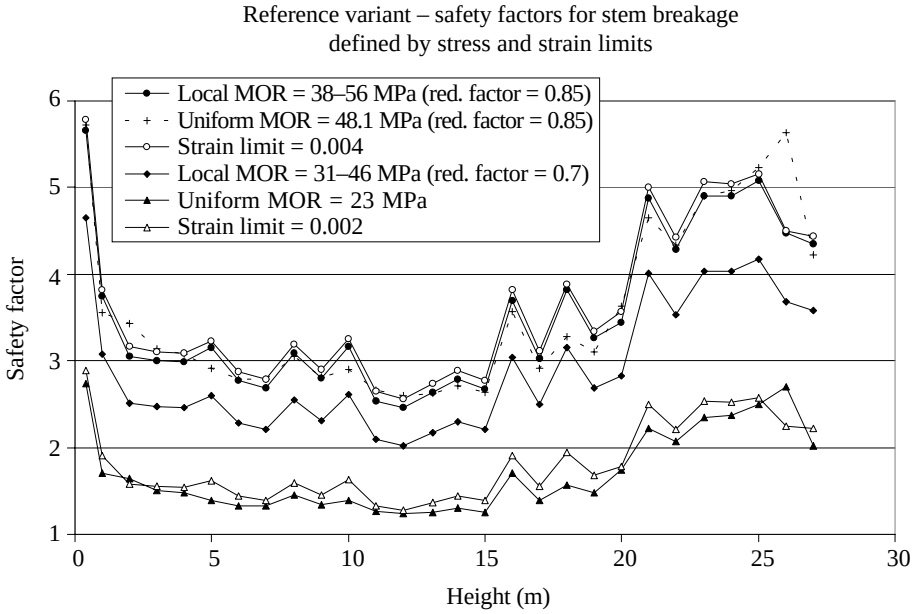

Fig. 12. Safety reserve against stem breakage, referring to differently defined limits – reference variant (S_Ref + C_Ref + W_Ref)

stem is reduced by 30% (FONS, PONG 1957; PETTY, WORRELL 1981; PELTOLA, KELLOMÄKI 1993) or by 15% (PELTOLA et al. 1999).

Referring to the breaking strength, for the investigated Douglas fir tree, a mean literature value of 48 MPa for green wood (with $\rho_0 = 0.47 g/cm^3$) was chosen (KOLLMANN 1951). Reduced by a factor of 0.85 and corrected by the locally measured wood densities (in the range from $\rho_0 = 0.44$ g/cm³ to 0.65 g/cm³), the estimated breaking strength varies between 38 and 56 MPa. A reduction factor of 0.7 results correspondingly in values from 31 to 46 MPa. If, simplified, an average density of the stem (0.55 g/cm³) is regarded, then the strength limit is uniform 48 MPa (reduction factor of 0.85). In a further variant, a very low, uniform limit of 23 MPa is chosen according to WESSOLLY and ERB (1998). (The value of 20 MB, proposed by the authors, was adjusted due to the assumed higher MOE of the tree.)

In comparison to strength data, values for strain parallel to grain at the proportional limit for green wood are seldom published. For Douglas fir, WESSOLLY and ERB (1998) state a strain proportional limit of 0.002, measured in compression. According to the U.S.D.A Forest Products Laboratory (1989), values for compression perpendicular to grain range from 0.0024 to 0.0029 for green wood and from 0.0041 to 0.005 for wood at a moisture content of 12%. YLINEN (1942, 1952) published a value of 0.004 for compression parallel to grain (Scots pine, dry sample).

Thus, according to differently chosen strength and strain limits and reduction factors, the remaining minimum safety factor, which is always located mid-stem at a height of uniform 12 m, varies from 1.2 (referring to the limit strength given by WESSOLLY and ERB [1998]) to 2.0 (reduction factor 0.7) or 2.6 (reduction factor 0.85) (Fig. 12).

DISCUSSION

Model validation: When drawing conclusions from the above-given simulations, it must always be born in mind that the outcome of the model could not be verified by data measured on a real, elastically reacting tree. Therefore, at least, it was desirable to compare the results of two quite different models, the finite element model (GAFFREY et al. 2001) and TREEFLEX, the holistic approach, by checking corresponding stress prognoses for inconsistencies, which could reflect principal model bugs. In this way, some errors (in both models) were found and removed. Remaining differences (Fig. 4) could not be attributed to any further possible errors, because not completely met was the necessary precondition of absolutely equal modelling in both geometry and material properties of tree and acting forces. Especially model divergences of the uppermost stem part could account for the observed stress differences, because the thinner the stem the greater will be the influence of changes in the cross-sectional form and absolute area of the stem, and of the forces. Thus, as prognosticated stress values cannot claim full validity, more importance is to be attached to their magnitude and the pattern of their distribution. In this sense, comparing both model approaches, it turns out that both trends for the vertical stress distribution coincide fairly well, which justifies the interpretation of the simulation results. Nevertheless, for a satisfying model verification, simultaneously measured data of wind and fibre strain (BLACKBURN 1997; BLACKBURN, GARDINER 1997) remain desirable.

The convergence of discretising and solving the differential equation system was successfully proven exemplarily. For the reference variant, the increase of supporting points from 9 to 17, to 33, and to 65 results in a change of the stem deflection (in, e. g., *x*-direction) of 6.6 cm, 1.0 cm and 0.3 cm maximum, respectively. The value of 6.6 cm found at 27 m is very little compared to the total deflection of 246 cm at that height. The numerical solution of the discretised equation system, using a Newton method, failed only in one case when a very high snow load on the light crown was combined with a high wind speed, resulting in an extreme deflection. (This simulation variant was, therefore, omitted.)

Hollow stems: Among all variants concerned with stem properties, the inner decomposition of a stem has the greatest effect on the stability of a tree. In the case of failure, in forest stands, this defect means economical loss but, e. g., in municipal locations, the endangering of public safety is the predominant aspect. As protection and preservation of old and big trees, which are often predestined to be hollow, is another declared public aim, experts are confronted with the dilemma deciding whether to fell or not to fell risk trees.

A simple, practical guideline is to spare those trees from felling which have a ratio of a remaining wall thickness to cross-section radius of more than 0.3 (MATTHECK et al. 1993; MATTHECK, BRELOER 1994). According to extensive surveys, such trees normally show sufficient resistance even in the heaviest storms. On the other hand, such a rigidly defined limit can imply the unnecessary removal of a high number of stable trees, too (SINN 1993; WESSOLLY 1993, 1995; WESSOLLY, ERB 1998), because trees with ratios of 0.1, or even less, can survive in storms. However, the stability of a tree must be analysed in combination with the state of the crown, which is mainly responsible for the received wind forces. It is argued that the bending resistance of a hollow stem with a wall/radius ratio of 0.3 is reduced only by about 25% (WESSOLLY 1995), but it must be emphasised that the per cent stress increase will be, as shown for the investigated Douglas fir, two times higher (Fig. 6d). Further reducing the supporting wall causes an exponential stress increase (MATTHECK, BRELOER 1994; SPATZ 1994), which can be confirmed, too: if the ratio is 0.1, for the diameter at breast height, the bending stiffness is reduced by 61% compared to the solid reference stem, but the stress increases from 13.5 MPa to 49.6 MPa (+270%) (Table 1). This indicates that the external bending moment does not remain constant; it must have increased from about 46 kNm to 65.5 kNm (at breast height) because, in the case of assuming constancy of the bending moment, a stress of only 35 MPa

(+160%) would be expected. Responsible is the horizontal shift of stem and crown masses and thus, the prolongation of the lever arms of the gravitational forces (Fig. 1): e. g., compared to the reference variant, the deflection of the stem in the south-east direction at a height of 27 m increases from 3.7 m to 10.3 m.

Lastly, it shall be mentioned that conventional calculating of the mechanical stability is justified in the case of hollow stems, too (SPATZ et al. 1990; SPATZ 1994). Hollow stems with a wall thickness to a radius ratio greater than 0.1 do not show a significant ovalisation of the cross section and thus, the reduction of the axial second moment of area need not be taken into account.

Further stem properties: Compared to hollowness, the influence of other geometry or material properties of the stem extremely falls off, though it cannot always be neglected. For example, the ability to form reaction wood under constant (wind) forces results in oval stem cross sections which have, with respect to the wind direction, a higher axial second moment of area than a circular cross section equal in area. The gained stress reduction, of up to 10%, as shown in Fig. 5, would probably be greater, if the formed compression wood, its distribution and its mechanical properties, could have been taken into account in the model.

A uniform horizontal distribution of the moisture content, as well as of the wood density, affect little if the chosen values do not differ too much from the averaged ones, which are derived by the non-uniform distribution models. The differences in stem mass, in mass distribution and in MOE distribution will alter the stresses only to a minor extent. Therefore, the application of such considerably simplified models seems legitimate. Greater deviations, e. g., the simulated 20% underestimation of wood density and MOE, cause increased stresses and especially much higher strains because the softer material deflects much more under a given load. For this reason, as the stem wood of many trees or tree species show a significant vertical change in density (and MOE) (spruce, pine, birch: YLINEN 1952; spruce: BRÜCHERT et al. 2000; *Cryptomeria japonica*: KATO, NAKATANI 2000), this variation should be assessed – even in the case of tree species, as Douglas fir, which normally do not show such a trend, because the density variation between neighbouring stem sections can be very great (GAFFREY, SLOBODA 2001).

Crown properties and wind forces: The wind forces acting on the crown depend on several factors: the wind velocity and the wind profile, on the one hand, and the sail area and the drag coefficient of the crown, on the other. As the pattern of wind profiles in a stand is very individual and can reliably be defined only by measurements (AMTMANN 1986), in most simulations, trees are assumed to stand solitary in order to allow the application of theoretical profiles (PELTOLA et al. 1999; GARDINER et al. 2000; SPATZ, BRÜCHERT 2000), such as the potential or the commonly preferred logarithmic profile. If their parameters are correspondingly chosen for a given case, the derived absolute and, in particular, relative stress distributions on the surface of the stem differ little in comparison to the one which is induced by a (hypothetical) within-stand wind profile (Fig. 11b). This demonstrates the importance of knowing in detail the acting wind forces, if, e. g., for a tree in a stand, the phenomenon of adaptive growth, i. e., the relationship between experienced stresses or strains and growth in diameter, shall be studied (GAFFREY, SLOBODA 2001).

The wind load on a crown is proportional to its sail area and to its drag coefficient. But the problem is the streamlining effect: both factors are reduced with increasing wind speed. To allow simplified modelling, either the sail area is held constant (WALSHE, FRASER 1963; MAYHEAD 1973) and the drag coefficient is variable, or vice versa (PELTOLA, KELLOMÄKI 1993). Unfortunately, applying both methods with the proposed parameters does not at all lead to congruent results (Fig. 11a). Indeed, it is hardly realisable or even impossible to accurately determine a function for the sail area or the drag coefficient reduction for an individual tree. Applying literature data will always remain very uncertain in view of the highly differing tree-specific crown properties.

Distribution of masses and gravitational forces: Though the mass of the stem is usually several times the mass of the crown (in the case of the studied tree: 920 kg vs. 220 kg), gravity forces of the latter contribute in greater part to the acting bending moments, at least in the upper half of the stem (PELTOLA, KELLOMÄKI 1993), because these masses, which are never symmetrically distributed with respect to the axis of the stem, are located more outward. If trees are leaning instead of standing upright, stresses can considerably be increased, too (SPATZ, BRÜCHERT 2000). In the above given example of the one-sided damaged, asymmetric crown (Fig. 9) stresses can locally be higher by 25%. Lastly, the effect of the localisation of masses on bending stresses is demonstrated by shifting the centroids of snow masses from midbranch to a more peripheral position (Fig. 10b).

It was supposed that the angles of the main branches have great influence on the stability of the tree: the masses of branches that hang downward should result in restoring bending moments, which counteract the bending of the tree (MÖHRING 1980, 1981). This could not be confirmed; the modification of the branch angles shows nearly no effect (Fig. 9). As very high wind forces were acting in this simulation, the effect of the crown-mass related gravity forces might be secondary and masked. However, in the absence of wind and if a heavy snow load (750 kg) covers the crown, the tree with obtuse branch angles is indeed remarkably more stable: stresses are reduced by 50% and more (Fig. 10a).

Safety against fracture: Here, safety is considered only as stability against snapping of the stem and not as stability against tree overturning, which might be less (PELTOLA et al. 1993, 1997). Prestresses, which enhance the safety of stem breakage to a great extent, are not taken into account, because measured values are missing and estimations are tainted with great uncertainty. Therefore,

the calculated safety factors underestimate the true safety reserve.

In the variants presented in Fig. 12, at first view, striking are the enormous differences in calculated minimum safety factors, which range from a critical value of 1.2 to a quite sufficient one of 2.6. But this must be seen in perspective with the purpose of defining the strength limits that are applied in the variants. The reference value of 48 MPa for maximum breaking stress in bending, the reduction factors of 0.7 or 0.85, and the proportional strain limit of 0.004 are given just as they are expected to represent the limit of fibre crushing. In contrast, the values of WESSOLLY and ERB (1998) contain a "safety supplement" because these published data are used by publicly appointed tree experts who have to evaluate the risk that emanates from a tree. The safety supplement shall avoid or, at least, minimise incorrect decisions that trees, which are expected to be safe, fail and cause damage, which could give rise to possible recourses. Moreover, in practise, taking wood samples to determine mechanical properties is normally too expensive, if, at all, allowed because of injuring the tree. Alternatively, strength data are taken from literature and therefore, these should be the lowest values. In this sense, instead of the crushing strength in bending, the lower one in compression (20 MPa) was published (WESSOLLY, ERB 1998). Correspondingly, a strain limit of 0.002 was chosen, which indicates the beginning of plastic deformation under compression, but not the point of fibre breakage.

Regarding the question of whether breaking stress or strain at the proportional limit shall be used as a reference, the advantage of the latter is its much lower variation (YLINEN 1942; WESSOLLY 1995; WESSSOLLY, ERB 1998). Indeed, the variation of the wood density and thus, of the derived breaking strength is also high for Douglas fir (SLOBODA, GAFFREY 1999; GAFFREY, SLOBODA 2001). If this vertical variability of the MOE is taken into account, the curve of the stress-based relative safety coincides very well with the one which is determined by the limit strain (Fig. 12, reduction factor 0.85). But, on the other hand, relating the estimated stresses to an average breaking strength instead of to locally calculated ones usually does not cause great differences but at single locations (e. g., at 17 m and 26 m). Therefore, the use of mean strength values as a reference seems to be justified, too.

The above made safety estimations only account for short-term loadings as it is the case for wind forces. If considerable snow masses remain on the crown for a longer time, the breaking strength is remarkably reduced. As the wood structure will plastically deform (creeping) under long-term loading, the final break will take place at about 50% of the value under short-term loading (HALL 1967; WORRELL 1979; PETTY, WORRELL 1981). Regarding the snow-loaded Douglas fir tree in the absence of wind, the tree will still be far away from any risk of stem breakage (Fig. 10a). But as soon as a heavy wind blows, the stem is supposed to snap somewhere at the height between 15 and 20 m (Fig. 10b). In combination with wind, it is the gravity force of the snow masses that is mainly responsible for the bending stresses (70–80%), whereas the stress contribution of the wind is 10–20%, of the branch masses 5–7%, and of the stem mass only 0–2%. Comparable results are given by PELTOLA et al. (1997).

As severe snow damage disasters occur more or less regularly, aspects of evaluating and improving the stability of single trees or entire stands under snow and wind loads have intensely been discussed (MÖHRING 1980; PETTY, WORRELL 1981; ROTTMANN 1985; MARSCH 1989; PELTOLA [ed.] 2000). Stem taper is the most important influencing characteristic: trees with a taper of 1:120, and still of 1:100, are considered to be very unstable (PELTOLA et al. 1997). For example, for young spruce (data were derived from a 14-year old tree), the risk of stem failure, by calculating the Euler buckling load, is estimated to be much higher (MARSCH 1989): already in the absence of wind, snow masses of 50 kg/m^2 can cause buckling of stems with a taper of even 1:80 or 1:90. But it must be pointed out that for the young spruce trees, the assumed mass relations of branch mass to stem mass to snow mass are 1:2.2:9.3 (calculated by the averaged masses for the taper of 1:80 and of 1:90) whereas, e. g., for the 64-year old Douglas fir tree with a taper of 1:86, the relations are 1:4:3.4. The much higher proportion of snow mass on the spruce crown will explain that buckling is already a risk at wind calm. Apart from the slenderness of the stem, the safety of the stem is influenced by crown characteristics (ROTTMANN 1985; MARSCH 1989) which determine, among other aspects, the amount and the distribution of the accrued snow masses. Crown asymmetries usually increase the risk of failure (Figs. 8, 9) whereas obtuse branch angles stabilise the tree (at least in the absence of wind) (Fig. 10a): down-hanging and snow-burdened branches produce a considerable restoring moment, which counteracts the bending of the stem. In this sense, the results of MÖHRING (1980, 1981), which were derived by applying a relatively simple two-dimensional Euler tree model, are verified.

References

AMTMANN R., 1986. Dynamische Windbelastung von Nadelbäumen. Schriftenreihe d. Forstwiss. Fakultät d. Univ. München u. d. Bay. Forstl. Versuchs- u. Forschungsanstalt, *74*: 215.

BARGMANN B.A., 1904. Die Verteidigung und Sicherung der Wälder gegen die Angriffe und die Gewalt der Stürme unter besonderer Berücksichtigung der örtlichen Windablenkungen. Allg. Forst.- Jagdztg, *82*: 81–89, 121–139, 161–177, 201–216, 241–257.

BAUMANN R., 1922. Die bisherigen Ergebnisse der Holzprüfungen in der Materialprüfungsanstalt der Technischen Hochschule Stuttgart. Forsch. Ing.-Wes., H. 231, Berlin.

BLACKBURN G.R.A., 1997. The growth and mechanical response of trees to wind loading. [PhD. Thesis.] Univ. of Manchester, Faculty of Science: 216.

BLACKBURN G.R.A., GARDINER B.A., 1997. The growth response of Sitka spruce to changes in wind loading. In: JERONIMIDIS G., VINCENT J.F.V. (eds.), Plant Biomechanics Conference 1997, Reading. Proc. II: posters: 43–44.

BRÜCHERT F., BECKER G., SPECK T., 2000. The mechanics of Norway spruce [*Picea abies* (L.) Karst.]: mechanical properties of standing trees from different thinning regimes. For. Ecol. Manag., *135*: 45–62.

COUTTS M.P., GRACE J. (eds.), 1995. Wind and trees. University Press, Cambridge: 485.

FONS L., PONG W.Y., 1957. Tree breakage characteristics under static loading – Ponderosa pine. U.S. Dept. Agr. For. Serv. Interim Tech. Report AFSWP – 867.

FOURCAUD T., LAC P., 1996. Mechanical analysis of the form and internal stresses of a growing tree by the finite element method. In: ENGIN A.E. (ed.), Bioengineering. PD-Volume *77*, Proc. of the 1996 Engineering Systems Design and Analysis Conference, Volume *5*, ASME 1996: 213–220.

FRIDMAN J., VALINGER E., 1998. Modelling probability of snow and wind damage using tree, stand and site characteristics from *Pinus sylvestris* sample plots. Scand. J. For. Res., *13*: 348–356.

GAFFREY D., 2000. Stress distribution in a stem of a 64-year old Douglas fir simulated with a 3D-tree and load model. In: SPATZ H.-C., SPECK T. (eds.), Plant Biomechanics 2000, Proc. of the 3rd Plant Biomechanics Conference Freiburg – Badenweiler, 27.8. –2.9.2000. Stuttgart, Georg Thieme Verlag: 425–431. [PDF file: www.uni.gaffrey.de]

GAFFREY D., HAPLA F., SABOROWSKI J., WAGNER B., MEGRAW R.A., 1999. Modellansätze zur Prognose der Rohdichteverteilung bei der Douglasie. Drev. Výsk., Bratislava, *44*(3–4): 39–59. [PDF file: www.uni.gaffrey.de]

GAFFREY D., RAABE K.-H., GEBBEKEN N., 2001. Untersuchungen zur Elastomechanik bei Douglasie. I. Modellierung mit der Finite-Elemente-Methode. Allg. Forst.- Jagdztg, *172*(5–6): 101–116. [PDF file: www.uni.gaffrey.de]

GAFFREY D., SABOROWSKI J., 1999. RBS, ein mehrstufiges Inventurverfahren zur Schätzung von Baummerkmalen. I. Schätzung von Nadel- und Asttrockenmassen bei 66-jährigen Douglasien. Allg. Forst- Jagdztg, *170*: 177–183. [PDF file: www.uni.gaffrey.de]

GAFFREY D., SLOBODA B., 2001. Tree mechanics, hydraulics and needle-mass distribution as a possible basis for explaining the dynamics of stem morphology. J. For. Sci., *47*: 241–254. [PDF file: www.uni.gaffrey.de]

GARDINER B. A., PELTOLA H., KELLOMÄKI S., 2000. Comparison of two models for predicting the critical wind speeds required to damage coniferous trees. Ecol. Modell., *129*: 1–23.

GARDINER B.A., QUINE C.P., 2000. Management of forests to reduce the risk of abiotic damage – a review with particular reference to the effects of strong winds. For. Ecol. Manag., *95*: 261–277.

GARDINER B.A., STACEY G.R., BELCHER R.E., WOOD C.J., 1997. Field and wind tunnel assessments of the implications of respacing on tree stability. Forestry, *70*(3): 233–252.

HÄCKEL H., 1993. Meteorologie. Stuttgart, Ulmer Verlag: 402.

HALL C.S., 1967. Some mechanical and nutritional aspects of cambial increment distribution in red pine. [PhD. Thesis.] Yale University, School of Forestry.

KATO A., NAKATANI H., 2000. An approach for estimating resistance of Japanese cedar to snow accretion damage. For. Ecol. Manag., *135*: 83–96.

KING D.A., 1986. Tree form, height growth, and susceptibility to wind damage in *Acer saccharum*. Ecol., *67*: 980–990.

KING D., LOUCKS O.L., 1978. The theory of tree bole and branch form. Radiat. Environ. Biophys., *15*: 141–165.

KOLLMANN F., 1951. Technologie des Holzes und der Holzwerkstoffe. Berlin, Springer: 1050.

LANDSBERG J.J., JAMES G.B., 1971. Wind profiles in plant canopies: studies on an analytical model. J. Appl. Meteorol., *8*: 729–741.

LANDSBERG J.J., JARVIS P.G., 1973. A numerical investigation of the momentum balance of a spruce forest. J. Appl. Ecol., *10*: 645–655.

MARSCH M., 1989. Biomechanische Modelle zur Quantifizierung der Tragfähigkeit von Einzelbäumen und Beständen gegenüber Schnee- und Windbelastung sowie darauf aufbauende Bestandesbehandlungsmaßnahmen mit Hilfe eines Simulationsmodells, dargestellt am Beispiel der Fichte. [PhD. Thesis.] Fakultät f. Bau-, Wasser- u. Forstwesen der Techn. Univ. Dresden, Dresden: 384.

MATTHECK C., 1990. Why they grow, how they grow: The mechanics of trees. Arboricult. J., *14*: 1–17.

MATTHECK C., 1991. Trees: the mechanical design. Berlin, Springer.

MATTHECK C., BETHGE K., ERB D., 1993. Failure criteria for trees. Arboricult. J., *17*: 201–209.

MATTHECK C., BRELOER H., 1994. Handbuch der Schadenskunde von Bäumen: Der Baumbruch in Mechanik und Rechtsprechung. Rombach, Freiburg i. Br.

MAYHEAD G.J., 1973. Some drag coefficients for British forest trees derived form wind tunnel studies. Agric. Meteorol., *12*: 123–130.

MCMAHON T.A., KRONAUER R.E., 1976. Tree structures: deducing the principle of mechanical design. J. Theor. Biol., *59*: 443–446.

METZGER C., 1893. Der Wind als maßgebender Faktor für das Wachsthum der Bäume. Mündener Forstl. Hefte, *5*: 35–86.

MILLER D.R., DUNHAM R., BROADGATE M.L., ASPINALL R.J., LAW A.N.R., 2000. A demonstrator of models for assessing wind, snow and fire damage to forests using the WWW. For. Ecol. Manag., *135*(1–3): 355–363.

MÖHRING B., 1980. Über die Zusammenhänge zwischen Baumform und Schneebruchanfälligkeit bei der Fichte. [Diploma Thesis.] Forstl. Fakultät der Univ. Göttingen, Göttingen: 77.

MÖHRING B., 1981. Über den Zusammenhang zwischen Kronenform und Schneebruchanfälligkeit bei Fichte. Forstarchiv, *4*: 130–134.

MOSBRUGGER V., 1990. The tree habit in land plants: a functional comparison of trunk constructions with a brief introduction into the biomechanics of trees. Berlin, Springer: 161.

NIKLAS K.J., 1992. Plant biomechanics. An engineering approach to plant form and function. The University of Chicago Press, Chicago: 607.

NIKLAS K.J., 1994. Interspecific allometries of critical buckling height and actual plant height. Am. J. Bot., *81*(10): 1275–1279.

NIKLAS K.J., 1997. Mechanical properties of Black Locust (*Robinia pseudoacacia*) wood: correlations among elastic and rupture moduli, proportional limit and tissue density and specific gravity. Ann. Bot., *79*: 479–485.

NIKLAS K.J., SPATZ H.-C., 1999. Methods for calculating factors of safety for plant stems. J. Exp. Biol., *202*: 3273–3280.

NIKLAS K.J., SPATZ H.-C., 2000. Wind-induced stresses in cherry trees: evidence against the hypothesis of constant stress levels. Trees, *14*(4): 230–237.

PALKA L.C., 1973. Predicting the effect of specific gravity, moisture content, temperature and strain rate on the elastic properties of softwood. Wood Sci. Techn., *7*: 127–141.

PELTOLA H. (ed.), 2000. Wind and other abiotic risks to forests. For. Ecol. Manag., *135*(1–3): 363.

PELTOLA H., KELLOMÄKI S., 1993. A mechanistic model for calculating windthrow and stem breakage of Scots pines at stand edge. Silva Fenn., *27*: 99–111.

PELTOLA H., KELLOMÄKI S., HASSINEN A., LEMETTINEN M., AHO J., 1993. Swaying of trees as caused by wind: analysis of field measurements. Silva Fenn., *27*(2): 113–126.

PELTOLA H., KELLOMÄKI S., VÄISÄNEN H., IKONEN V.-P., 1999. A mechanistic model for assessing the risk of wind and snow damage to single trees and stands of Scots pine, Norway spruce, and birch. Can. J. For. Res., *29*: 647–661.

PELTOLA H., NYKÄNEN M.-L., KELLOMÄKI S., 1997. Model computations on the critical combination of snow loading and windspeed for snow damage of Scots pine, Norway spruce and Birch sp. at stand edge. For. Ecol. Manag., *95*: 229–241.

PETTY J.A., WORRELL R., 1981. Stability of coniferous tree stems in relation to damage by snow. Forestry, *54*: 115–128.

QUINE C.P., 1998. Strong winds forecast. For. Brit. Timber, *27*(2): 12–16.

ROTTMANN M., 1985. Schneebruchschäden in Nadelholzbeständen. Beiträge zur Beurteilung der Schneebruchgefährdung, zur Schadensvorbeugung und zur Behandlung schneegeschädigter Nadelholzbestände. Frankfurt a. M. J.D. Sauerländer's Verlag.

SINN G., 1993. Grundsätzliches zur Bruchsicherheit von Bäumen. Eine Argumentationshilfe in Schadenersatzfällen. Das Gartenamt, *42*(6): 387–392.

SLOBODA B., GAFFREY D., 1999. Dynamik der Stammorphologie. Abschlußbericht zum DFG-Projekt Sl 11/6-1: 95. [PDF file: www.uni.gaffrey.de]

SPATZ H.-C., 1994. Ein Kommentar zur mechanischen Stabilität hohler Bäume. Das Gartenamt, *43*(2): 92–95.

SPATZ H.-C., BRÜCHERT F., 2000. Basic biomechanics of self-supporting plants: wind loads and gravitational loads on a Norway spruce tree. For. Ecol. Manag., *135*: 33–44.

SPATZ H.-C., SPECK T., VOGELLEHNER D., 1990. Contributions to the biomechanics of plants. II. Stability against local buckling in hollow plant stems. Botanica Acta, *103*: 123–130.

SPECK T., 1994. Bending stability of plant stems: ontogenetical, ecological, and phylogenetical aspects. Biomimetics, *2*: 109–128.

SPECK T., SPATZ H.-C., VOGELLEHNER D., 1990. Contributions to the biomechanics of plants. I. Stabilities of plant stems with strengthening elements of different cross-sections against weight and wind forces. Botanica Acta, *103*: 111–122.

SPECK T., ROWE N. P., BRÜCHERT F., HABERER W., GALLENMÜLLER F., SPATZ H.-C., 1996. How plants adjust the "material properties" of their stems according to differing mechanical constraints during growth: an example of smart design in nature. Proc. of the 1996 Engineering Systems Design and Analysis conference, Vol. *5*, Bioengineering, The American Society of Mechanical Engineers, PD-Vol. *77*: 233–241.

STERCK F.J., BONGERS F., 1998. Ontogenetic changes in size, allometry, and mechanical design of tropical rain forest trees. Am. J. Bot., *85*(2): 266–272.

SZABÓ I., 2001. Höhere technische Mechanik. 6. Aufl., Berlin, Springer Verlag.

TALKKARI A., PELTOLA H., KELLOMÄKI S., STRANDMAN H., 2000. Integration of component models from the tree, stand and regional levels to assess the risk of wind damage at forest margins. For. Ecol. Manag., *135*(1–3): 303–313.

TIMOSHENKO S.P., 2000. Theory of elastic stability. 2nd ed., New York, McGraw-Hill.

TIRÉN L., 1928. Einige Untersuchungen über die Schaftform. Mitteilungen aus der Forstl. Versuchsanstalt Schwedens, *24*: 81–152.

U.S.D.A. Forest Products Laboratory (1989). Handbook of wood and wood-based materials for engineers, architects, and builders. Hemisphere Publishing Corp., New York.

VALINGER E., FRIDMAN J., 1997. Modelling probability of snow and wind damage in Scots pine stands using tree characteristics. For. Ecol. Manag., *97*: 215–222.

VINCENT J.F.V., 1990. Structural biomaterials. Princeton, Princeton University Press.

WAINWRIGHT S.A., BIGGS W.D., CURREY J.D., GOSLINE J. M., 1976. Mechanical designs in organisms. London, Edward Arnold: 422.

WALSHE D.E., FRASER A.I., 1963. Wind-tunnel tests on a model forest. NPL Aero Rep. 1078, Nat. Physical Lab., Aerodynamics Division, London.

WESSOLLY L., 1993. Stand- und Bruchsicherheit von Bäumen. Leistungsfähigkeit und Grenzen der Zugversuche. Das Gartenamt, *42*(8): 486–491.

WESSOLLY L., 1995. Bruchdiagnose von Bäumen. Teil 1: Statisch integrierte Verfahren – Messung mit Zugversuch. Die Diagnosemethode des Sachverständigen. Stadt und Grün, *44*(6): 416–423.

WESSOLLY L., ERB M., 1998. Handbuch der Baumstatik und Baumkontrolle. Berlin, Patzer Verlag.

WILSON B.F., ARCHER R.R., 1979. Tree design: some biological solutions to mechanical problems. Biosci., *29*(5): 293–298.

WORRELL R., 1979. Snow damage to the stems of coniferous trees. [PhD. Thesis.] Dep. of Agricult. and Forestry, Univ. of Aberdeen: 132.

YLINEN A., 1942. Über den Einfluß der Probekörpergröße auf die Biegefestigkeit des Holzes. Holz als Roh- und Werkstoff, *5*(9): 299–305.

YLINEN A., 1952. Über die mechanische Schaftformtheorie der Bäume. Technische Hochschule in Finnland. Wiss. Forsch., *7*: 51.

Received 3 December 2001

APPENDIX

CONCEPTION OF MODELLING TREE ELASTOMECHANICS

Required background information is given in the preceding paragraphs. In the following, for convenience, a vectorial notation of the mathematical terms is chosen.

Bending and twisting of the stem

Each stem cross section A has a neutral point which is characterised by $\int_A E(\bar{x})\bar{x}\,dA = 0$ if the neutral point is set identical with the origin of a local Cartesian co-ordinate system (LCS). The cross section shall lie within the xy-plane of the LCS. $E(\bar{x})$ is the local modulus of elasticity and $\bar{x}$ is a point in A. A global co-ordinate system (GCS) is chosen with its origin in the neutral point of the lowest stem cross section (bottom of the tree) and with the z-axis vertically oriented. The course of the neutral fibre $\bar{r}(h)$ is defined in the CGS. In the absence of acting forces, the neutral fibre is not bent, vertical, and for any height h given by $\bar{r}(h) = h \cdot \bar{e}_z$. Torsion is defined by $\varphi(h)$ which is the angle on which the stem at h is rotated on its vertical axis. Torsion is assumed to be rigid, i. e., no distortion of the cross-sectional area shall exist and thus, the area shape remains invariant.

Acting forces

The description is reduced to point forces because volume forces (like gravitational forces of stem wood masses) can be approximated by a sufficient number of point forces. Each force $\bar{F}_i$, $i = 1,...,n$, acts at a height h_i on the stem and has a lever arm $\bar{l}_i$ with respect to the point of application. Regarding the gravitational force of a branch mass m_i, $\bar{l}_i$ is the distance from mid-branch (the assumed location of the mass centroid) to the neutral fibre (stem centre) and we have the force $\bar{F}_i = -m_i g \bar{e}_z$, where g is the gravitational constant. Lever arms be rigidly fixed to the stem and be correspondingly moved by stem bending. Forces do not depend on stem bending.

Elastostatic

Regarding any cross section, in the loading case, the LCS is shifted and rotated against the GCS. One condition for the rotation matrix $R(h)$ which transforms local co-ordinates to global ones is $R(h)\bar{e}_z = \bar{r}'/|\bar{r}'|$, where $\bar{e}_z$, the vertical in the LCS, describes the tangential direction in the GCS. Second, to include torsion $\varphi(h)$, we consider the direction of the bent neutral axis which is given by $\bar{r}'(h) \times \bar{r}''(h)$. In a simplified assumption, for all cross sections this direction shall not differ much and thus, being approximately horizontal, is given by $\bar{r}'(h) \times \bar{e}_z$. Without torsion, in the case of bending when the LCS is changed to the GCS, the direction of the bent neutral axis remains invariant. If torsion occurs, in the LCS, we rotate by $\varphi(h)$ in the opposite direction and demand invariance:

$$R(h)\,R_{\varphi(h)}^{-1}\left(\bar{r}'(h)\times\bar{e}_z\right) = \bar{r}'(h)\times\bar{e}_z, \quad R_{\varphi(h)} = \begin{pmatrix} \cos\varphi & -\sin\varphi & 0 \\ \sin\varphi & \cos\varphi & 0 \\ 0 & 0 & 1 \end{pmatrix}$$

The rotation matrix is

$$R(h) = \begin{pmatrix} 1-\dfrac{r_x'^2/\bar{r}'^2}{1+r_z'/|\bar{r}'|} & -\dfrac{r_x' r_y'/\bar{r}'^2}{1+r_z'/|\bar{r}'|} & \dfrac{r_x'}{|\bar{r}'|} \\ -\dfrac{r_x' r_y'/\bar{r}'^2}{1+r_z'/|\bar{r}'|} & 1-\dfrac{r_y'^2/\bar{r}'^2}{1+r_z'/|\bar{r}'|} & \dfrac{r_y'}{|\bar{r}'|} \\ -\dfrac{r_x'}{|\bar{r}'|} & -\dfrac{r_y'}{|\bar{r}'|} & \dfrac{r_z'}{|\bar{r}'|} \end{pmatrix} \cdot R_{\varphi(h)}$$

If $\bar{x} = (x, y, 0)$ is a point on a cross section A, $\bar{n} = (n_x, n_y, 0)$ a unit vector in the LCS in bending direction, and $k(h)$ the curvature of the stem at h then, the bending stress at $\bar{x}$ is $\sigma(\bar{x}) = k(h)E(\bar{x})(\bar{n}\bar{x})$, and acting on an infinitesimal area dA are the force $d\bar{F} = \sigma(\bar{x})\bar{e}_z dA$ and the bending moment $d\bar{T}_B = \bar{x} \times d\bar{F} = (\bar{x} \times \bar{e}_z)\, kE(\bar{x})\, (\bar{n}\bar{x})\, dA$. As for the total cross-sectional area,

$$\begin{aligned} \bar{T}_B(h) &= \int_A d\bar{T} = \int_A (\bar{x}\times\bar{e}_z)\, kE(\bar{x})\, (\bar{n}\bar{x})\, dA \\ &= k(h) \begin{pmatrix} \int_A E(\bar{x})xy\,dA & \int_A E(\bar{x})y^2\,dA & 0 \\ -\int_A E(\bar{x})x^2\,dA & -\int_A E(\bar{x})xy\,dA & 0 \\ 0 & 0 & 0 \end{pmatrix} \\ &=: k(h)\,S(h)\,\bar{n} \end{aligned}$$

The matrix $S(h)$ describes the flexural stiffness at h, which depends on the bending direction. The unit vector $\bar{n}$ in bending direction is $\bar{n} = R(h)^{-1}\bar{r}''/|\bar{r}''|$ because, in the GCS, $\bar{r}''$ points in this direction. The curvature $k(h)$ is known by

$$k(h) = \sqrt{\frac{\bar{r}'^2\,\bar{r}''^2 - \left(\bar{r}'\,\bar{r}''\right)^2}{\left(\bar{r}'^2\right)^3}}$$

The bending strain is superposed by a strain $\varepsilon(h) = |\bar{r}'(h)| - 1$ which is constant within the cross section and which results in a vertical force $dF = -\varepsilon(h)E(\bar{x})\,dA$ on the

infinitesimal area dA and in a total strain force

$$F_S = -\varepsilon(h)\int_{dA} E(\bar{x})\,dA =: -\varepsilon(h)D(h) \text{ on } A.$$

The rigid rotation on $\varphi(h)$ causes a further torsional moment $\bar{T}_T = -D_T(h)\varphi'(h)\,\bar{e}_z$, given in the LCS. $D_T(h)$ could be derived from the elastic moduli that are radial and tangential to the grain and the POISSON's constants. (As in the present state of the simulation software, torsion is not yet implemented, a detailed description is spared.)

State of equilibrium

The inner moment $R(h)\,(\bar{T}_B(h) + \bar{T}_T(h))$, resulting from bending and torsional moments, shall compensate the outer moment caused by all acting forces above h. If, for the i-th force, the lever arm (valid at h) is $\bar{r}(h_i) + R(h_i)\bar{l}_i - \bar{r}(h)$ then, the equilibrium is defined by

$$R(h)\left(\bar{T}_B(h) + \bar{T}_T(h)\right) + \sum_{\substack{i \\ h_i \geq h}} \left(\bar{r}(h_i) + R(h_i)\bar{l}_i - \bar{r}(h)\right) \times \bar{F}_i = 0 \qquad \text{(A)}$$

The force $F_S(h)$ caused by strain must equal those shares of all forces above h which are tangential to the curvature, i. e., having the direction $\vec{r}\,'/|\vec{r}\,'|$:

$$F_S(h) + \frac{\vec{r}\,'}{|\vec{r}\,'|} \cdot \sum_{\substack{i \\ h_i \geq h}} \bar{F}_i = 0 \qquad \text{(B)}$$

(A) and (B) set up a coupled differential equation system (DES) of the second order for $\bar{r}(h)$ and of the first order for $\varphi(h)$. As the stem shall rigidly be fixed in the ground, the initial conditions are

$$\bar{r}(0) = 0, \bar{r}'(0) = \bar{e}_z, \varphi(0) = 0$$

An explicit solution of this complex DES does not exist. Therefore, the stem is discretised into not necessarily equidistant segments at heights $t_j, j = 1,..., m$. Remaining variables of the DES are the values $\bar{r}(t_j)$ and $\varphi(t_j)$. Interpolations results in $\bar{r}'(t_j), \bar{r}''(t_j)$, and $\varphi'(t_j)$ and thus, we have a non-linear equation system for $(\bar{r}(t_j), \varphi(t_j))$ which is solved by a Newton algorithm. Starting values are taken from the unloaded tree.

Elasticko-mechanické vlastnosti douglasky tisolisté, její citlivost vůči faktorům ovlivňujícím dřeviny, větru a sněhovým zátěžím, a důsledky pro stabilitu – simulační studie

D. GAFFREY[1], O. KNIEMEYER[2]

[1]*Univerzita v Göttingenu, Fakulta lesnických věd a lesní ekologie, Ústav lesnické biometrie a informatiky, Göttingen, Německo*

[2]*Univerzita v Göttingenu, Fakulta fyziky, Ústav teoretické fyziky, Göttingen, Německo*

ABSTRAKT: Pro účely simulace elasticko-mechanických vlastností stromů vystavených větru a gravitačním silám jsme vyvinuli kompletní 3-D model s cílem vyhodnotit rozložení napětí a tlaku na povrchu kmene. Model jsme přizpůsobili geometrickým a fyzickým vlastnostem stromu douglasky tisolisté ve stáří 64 let. Ke studiu jejich vlivu na změnu napětí vlákna, a tedy na bezpečnostní rezervu proti zlomu kmene, jsme různým způsobem upravovali původní data týkající se kmene a koruny, jakož i aplikované síly.

Klíčová slova: douglaska tisolistá; elasticko-mechanický model; napětí; tlak; bezpečnostní rezerva; zlom kmene

Corresponding author:

Dr. DIETER GAFFREY, Georg-August-University of Göttingen, Faculty of Forest Sciences and Forest Ecology, Institute of Forest Biometry and Informatics, Büsgenweg 4, 37077 Göttingen, Germany
tel.: + 49(0)551 39 34 60, fax: + 49(0)551 39 34 65, e-mail: uni@gaffrey.de; http:// www.uni.gaffrey.de